

CONFIDENTIAL

Copy 5
RM L54B15

NACA RM L54B15

NACA

RESEARCH MEMORANDUM

A TRANSONIC WIND-TUNNEL INVESTIGATION OF THE EFFECTS OF
TWIST AND CAMBER WITH AND WITHOUT INCIDENCE, TWIST,
AND BODY INDENTATION ON THE AERODYNAMIC
CHARACTERISTICS OF A 45° SWEPTBACK
WING-BODY CONFIGURATION

CLASSIFICATION ~~CHANGED~~ ^{Revised} by Lawrence Cooper

To INCLASSIFIED Langley Aeronautical Laboratory
Langley Field, Va.

By authority of NASA TPA 7 ^{Effective} Date 5-29-59
US 7-7-59

CLASSIFIED DOCUMENT

This material contains information affecting the National Defense of the United States within the meaning of the espionage laws, Title 18, U.S.C., Sec. 793 and 794, the transmission or revelation of which in any manner to an unauthorized person is prohibited by law.

NATIONAL ADVISORY COMMITTEE FOR AERONAUTICS

WASHINGTON

April 1, 1954

CONFIDENTIAL

INCLASSIFIED

NATIONAL ADVISORY COMMITTEE FOR AERONAUTICS

RESEARCH MEMORANDUM

A TRANSONIC WIND-TUNNEL INVESTIGATION OF THE EFFECTS OF
TWIST AND CAMBER WITH AND WITHOUT INCIDENCE, TWIST,
AND BODY INDENTATION ON THE AERODYNAMIC
CHARACTERISTICS OF A 45° SWEEPBACK
WING-BODY CONFIGURATION

By J. Lawrence Cooper

SUMMARY

A transonic wind-tunnel investigation of several sweptback wing-body configurations has been made to determine the effects of twist and camber with incidence, the separate effects of twist without camber, and the influence of body indentation on the effects of twist and camber, and twist alone.

Comparisons of the results of this investigation with those obtained for comparable plane wing-body configurations showed: Negative incidence improved the values of maximum lift-drag ratios for the twisted and cambered wing-body configuration throughout the test Mach number range. The effects of twist on the values of maximum lift-drag ratios, however, were small when compared with those of twist and camber. Twisting and cambering the wing increased the lift coefficient at which the unstable break in the pitching-moment curves occurred by approximately twice the amount of that for twist alone. Body indentation increased the values of maximum lift-drag ratios for the twisted and cambered wing-body configuration at Mach numbers between 0.90 and 1.15 and increased the values of maximum lift-drag ratios for the twisted wing-body configuration through Mach number 1.03. The effects of twist and camber and body indentation at lift coefficients for maximum lift-drag ratios are additive at Mach numbers above 0.96.

INTRODUCTION

The results of reference 1 indicated that twist and camber increased the maximum lift-drag ratios of a 45° sweptback wing-curved-body

~~CONFIDENTIAL~~

UNCLASSIFIED

configuration at Mach numbers up to 0.84 and above 0.99 but reduced the $(L/D)_{\max}$ values between these Mach numbers. The twisted and cambered wing used in this investigation was designed in accordance with the prescribed method of reference 2 for the wing alone to have a uniform loading at a Mach number of 1.2 and a lift coefficient of 0.4. These previous tests were made with the body at an angle of 0° with respect to the wing design reference plane. It was reasoned that setting the body at a positive angle with respect to the design reference plane of the wing would produce a lift distribution for the combination that more nearly approached the distribution on the wing alone at the design conditions; this lift distribution might result in improved effectiveness of twist and camber. In order to determine the effect of twist and camber with the body set at a positive angle, the wing of reference 1 was tested at angles of incidence i_w of 0° and -4° (fig. 1) in combination with a basic body and the results compared with those of the comparable plane wing-body configuration with 0° incidence (ref. 3).

It would be of practical interest to know the separate contributions of twist and camber in the improvements in performance noted in reference 1. As an initial step in determining these individual contributions, a wing with the same twist as that of the wing of reference 1 but with no camber has been tested at an angle of incidence i_w of -4° and the results compared with those obtained with the comparable plane wing (ref. 3) and with the comparable twisted and cambered wing. This twist distribution is similar to that for an actual plane sweptback wing with aeroelastic deformation. Therefore, these data for a twisted wing provide information as to the effects of aeroelastic deformation. The effects of this same twist distribution on the loads on this wing are presented in reference 4.

The results of reference 5 indicated that body shape has a pronounced effect on the drag characteristics of a twisted and cambered 45° sweptback wing-body configuration at transonic speeds. Also, the results of reference 6 indicated that the interference effect between a plane sweptback wing and a body could be minimized at transonic speeds by indenting the body in the region of the wing on the basis of the transonic area rule (ref. 7). Therefore, it might be expected that indenting the body on the basis of the transonic area rule would improve the drag characteristics of a twisted and cambered or a twisted sweptback wing-body configuration. The twisted and cambered wing of reference 1 and the comparable twisted wing were tested with a basic body indented according to the transonic area rule for Mach number 1.00, and the results were compared with a comparable plane wing—indented-body configuration (ref. 3).

These tests were conducted in the Langley 8-foot transonic tunnel. With the exception of the maximum Mach number of the twisted wing with

the basic body being limited to 1.03, each wing-body configuration was tested through a continuous Mach number range from 0.80 to 1.03 and at a Mach number of approximately 1.15.

CONFIGURATIONS

Five sting-mounted wing-body configurations were tested. They consisted of a twisted and cambered wing without incidence tested in combination with a basic body, and a twisted and cambered wing and a twisted wing with incidence tested in combination with a basic body and the same basic body with indentation. A plan-form drawing of these wing-body configurations is presented in figure 1.

Each of the wings had 45° sweepback of the 0.25 chord line, an aspect ratio of 4, a taper ratio of 0.6, and NACA 65A-series airfoil sections 6 percent thick parallel to the plane of symmetry. The twisted and cambered wing was designed to obtain a uniform load distribution at a lift coefficient of 0.4 and a Mach number of 1.2 (ref. 1). The resulting twist and camber values are presented in figure 2, where the angle of twist was measured relative to the design reference plane of the wing. The twisted wing had a twist distribution identical to that of the twisted and cambered wing. The twisted and cambered wing was tested at angles of incidence of 0° and -4° whereas the twisted wing was tested only at an angle of incidence of -4° . As shown in figure 1, the angle of incidence i_w is the angle between the design reference plane of the wing and the body axis, and the angle β at any spanwise station is the angle between the chord line of the wing section at that station and the body axis. From figures 1 and 2, it is seen that the angle β for the twisted and cambered wing and the twisted wing at the wing-body junction is approximately 4.2° for 0° incidence and approximately 0.2° for -4° incidence.

The basic body and the indented body used in this investigation were the same bodies used with the comparable plane wing of reference 3. The indentation was such that the sum of the cross-sectional areas normal to the airstream for the indented body and the wing at each longitudinal station was equal to the cross-sectional area of the basic body normal to the airstream at the same station. The area developments of the wing-body configurations with the basic and the indented body are shown in figure 3, and the coordinates for the basic and the indented bodies are given in table I.

MEASUREMENTS, ACCURACY, AND CORRECTIONS

Lift, drag, and pitching moment were measured by an electrical strain-gage balance. The maximum estimated errors of the resulting coefficients are as follows:

C_L	± 0.01
C_D	± 0.001
C_m	± 0.004

The drag data have been adjusted for base pressures such that the drag corresponds to conditions for which the base pressure is equal to the free-stream static pressure. The base pressure coefficients were computed by the standard relation $P_b = \frac{P_b - P_o}{q_o}$, and the maximum estimated error in the resulting coefficients is ± 0.005 . The base pressure coefficients for the twisted, and twisted and cambered wing-body configurations with incidence are shown in figure 4. No corrections have been made to the base pressures for sting interference effects.

Local deviations from the average free-stream Mach numbers in the region of the model were no larger than 0.003 at subsonic speeds, and with increases in Mach number above 1.00 the deviations increased to the order of 0.010 at a Mach number of 1.15.

The angle of attack was measured by an electrical strain gage mounted in the nose of the model. A description of the angle-of-attack measuring system is given in reference 8, and as reported therein the measurements are believed to be accurate within $\pm 0.1^\circ$.

The effects of wall-reflected disturbances on the drag results are small at Mach numbers below 1.03 and negligible at Mach numbers above 1.145. No results were obtained for the range of Mach numbers from 1.03 to 1.145. No corrections for the effects of wall-reflected disturbances have been applied to the data.

PRESENTATION OF RESULTS

The basic aerodynamic data (body angle of attack, drag coefficient, and pitching-moment coefficient against lift coefficient) for the plane wing-body configurations (ref. 3), the twisted and cambered wing-body configurations without and with incidence, and the twisted wing-body configurations with incidence are presented in figures 5, 6, 7, and 8, respectively. The drag curves for the plane wing—basic-body configuration without incidence and the twisted and cambered wing—basic-body

configuration with and without incidence at lift coefficients of 0.05, 0.30, and 0.40 are shown in figure 9. Comparisons at several lift coefficients of the lift-drag ratios of the twisted and cambered wing-body configurations to those of the plane wing-body configurations

$\left[\frac{(L/D)_{\text{Twisted and cambered wing}}}{(L/D)_{\text{Plane wing}}} \right]$ are shown in figure 10

for the wing—basic-body configuration with and without incidence and the wing—indented-body configuration with incidence. Variations of the maximum lift-drag ratios with Mach number for the plane wing—basic-body configuration without incidence and the twisted and cambered wing—basic-body configuration with and without incidence are presented in figure 11. The drag curves for the plane, twisted, and twisted and cambered wing-body configurations with basic and indented bodies at lift coefficients of 0.05, 0.3, and 0.4 are shown in figure 12. Curves showing the effects of body indentation on the drag of the plane, twisted, and twisted and cambered wing-body configurations at lift coefficients of 0.05, 0.3, and 0.4 are shown in figure 13. Comparisons at several lift coefficients of the lift-drag ratios of the twisted wing-body configurations to those of the plane wing-body configurations

$\left[\frac{(L/D)_{\text{Twisted wing}}}{(L/D)_{\text{Plane wing}}} \right]$ are shown in figure 14 for both the

indented and basic bodies. Variations of the maximum lift-drag ratios with Mach number for the plane, twisted, and twisted and cambered wing-body configurations with indented and basic bodies are presented in figure 15, and the lift coefficients for maximum lift-drag ratios are shown in figure 16. The lift coefficients at which the break in the pitching-moment curves occurred for the plane, twisted, and twisted and cambered wing-body configurations with both the indented and basic bodies are shown in figure 17.

Because of the consistency of the data, the curves of $(L/D)_{\text{max}}$ (figs. 11 and 15) and lift coefficient for $(L/D)_{\text{max}}$ (figs. 11 and 16) were arbitrarily faired between Mach numbers 1.03 and 1.15.

In order to facilitate presentation of the data, staggered scales have been used in some of the figures and care should be taken in identifying the zero axis for each curve. The Reynolds number based on the mean aerodynamic chord varies from 1.83×10^6 to 2.00×10^6 .

DISCUSSION

Twist and Camber With Incidence

Drag coefficients.— From figure 9, it is seen that setting the twisted and cambered wing at -4° incidence, thereby setting the body at

a positive angle relative to the design reference plane of the wing, had the same general but greater effect of increasing the drag above that of the plane wing—basic-body configuration at a lift coefficient of 0.05 as the twisted and cambered wing with 0° incidence. However, this effect of the twisted and cambered wing with negative incidence was completely reversed at lift coefficients of 0.3 and 0.4. At these lift coefficients the wing with negative incidence reduced the drag throughout the test Mach number range, whereas the wing without incidence had little or no effect on the drag at Mach numbers between 0.93 and 1.03 and reduced the drag to a much lesser degree than the wing with negative incidence at Mach numbers below 0.93. Also, this figure shows that the reduction in drag for the wing with negative incidence increases with increase in lift coefficient.

Lift-drag ratios.— Figure 10 indicates that changing the angle of incidence from 0° to -4° had little influence on the effectiveness of twist and camber at 0.2 lift coefficient but increased its effectiveness throughout the Mach number range for lift coefficients of 0.3 to 0.5. At 0° incidence, twist and camber was only effective in significantly increasing the values of lift-drag ratios over that for the plane wing—basic-body configuration at Mach numbers below 0.93 and had little or no effect at Mach numbers above 0.93.

The maximum lift-drag ratios presented in figure 11 indicate that twist and camber with negative incidence significantly increased the values of maximum lift-drag ratios over those for the plane wing—basic-body configuration throughout the Mach number range, whereas twist and camber without incidence increased these values of maximum lift-drag ratios only at Mach numbers below 0.93.

For this investigation, the maximum increase in the values of maximum lift-drag ratios due to twist and camber with negative incidence was between Mach numbers 0.80 and 0.90. Then the improvements in the values of maximum lift-drag ratios decreased very rapidly with increase in Mach number up to 0.95 and from there on decreased slowly up to Mach number 1.15.

From these results, it would appear that the conjectures that led to this investigation of incidence, as stated in the introduction, are correct.

Pitching-moment coefficients.— A comparison of figures 5(c), 6(c), and 7(c) shows that twist and camber with negative incidence made the pitching-moment coefficients for the wing—basic-body configuration more positive throughout the Mach number range than twist and camber without incidence and more negative at low lift coefficients than the plane wing. Also, twist and camber with negative incidence increased the lift coefficient at which the unstable break in the pitching-moment curves occurred for the plane wing—basic-body configuration as shown in figure 17.

Twist

Drag coefficients.- Figure 12 shows that at a lift coefficient of 0.05 the effect of twist alone on the basic wing-body configuration was similar to that of twist and camber since it also increases the drag of the configuration throughout the Mach number range. However, at lift coefficients of 0.3 and 0.4, twist did not significantly decrease the drag of the configuration as was the case for twist and camber.

Lift-drag ratios.- Figure 14 indicates that twist had relatively small effects on the lift-drag ratios throughout the speed range at lift coefficients of 0.2 to 0.5. Also, as shown in figure 15, the effects of twist on the maximum lift-drag ratios were small compared with those of twist and camber.

Pitching-moment coefficients.- From figures 5(c) and 8(c), it is seen that the general effect of twist on the pitching-moment coefficients was different from that of twist and camber, for it made the pitching-moment coefficients for the wing-body configurations more positive throughout the Mach number and lift-coefficient ranges than the plane wing. Figure 17 shows that twist increased the lift coefficient at which the unstable break in the pitching-moment curves occurred by approximately one-half the amount of that for twist and camber.

Body Indentation

Drag coefficients.- From figure 12 it is seen that body indentation had little influence on the relative effects of twist and camber or twist on drag. Also, figure 13 shows that the reductions in drag associated with body indentation were generally roughly the same for the twisted and cambered, twisted, and plane wing-body configurations at lift coefficients of 0.05, 0.3, and 0.4. The effects of body indentation on drag were small at Mach numbers below 0.90, but the drag reduction increased with increase in Mach number until a maximum was reached at a Mach number of approximately 1.00. From Mach number 1.00 to 1.03, the drag reduction dropped off, and with further increase in Mach number tended to decrease slightly.

Lift-drag ratios.- The effectiveness of twist and camber in improving the lift-drag ratios (fig. 10) generally was roughly the same with the indented body and the basic body for lift coefficients from 0.2 to 0.4, but at a lift coefficient of 0.5 indentation definitely improved the effectiveness of twist and camber at Mach numbers below 0.93. As shown in figure 14, the influence of indentation on the effectiveness of twist was small at lift coefficients of 0.2 to 0.5.

Figure 15 shows that body indentation increased the values of maximum lift-drag ratios for the twisted and cambered wing-body configuration at Mach numbers between 0.90 and 1.15 and increased the values of maximum lift-drag ratios for the twisted and plane wing-body configurations throughout the test Mach number range. Below Mach number 1.00, indentation was somewhat more effective in increasing the values of maximum lift-drag ratios of the plane wing-body configuration than for the twisted wing-body configuration.

In figure 15 there is also presented a composite curve, the values of which were obtained by adding the difference in the values of maximum lift-drag ratios due to body indentation for the plane wing-body configuration to the values of maximum lift-drag ratios for the twisted and cambered wing-body configuration with the basic body. From this curve it is readily seen that the sum of the separate effects of body indentation and twist and camber is approximately the same as their combined effects at Mach numbers above 0.96.

As shown in figure 16 the addition of body indentation appreciably reduced the lift coefficient at which maximum lift-drag ratios occurred for Mach numbers above 0.96 for the twisted and cambered, twisted, and plane wing-body configurations. From Mach numbers 0.80 to 0.96, the reductions in lift coefficient were generally small for the configurations tested.

Pitching-moment coefficients.- From figures 7(c) and 8(c), it is seen that body indentation had little effect on the pitching-moment coefficients for the twisted and cambered, and twisted wing-body configurations, with the exception of a destabilizing effect at low lift coefficients for Mach numbers from 0.90 to 0.96. Also, these figures indicate that body indentation had no effect on the lift coefficient at which the unstable break in the pitching-moment curves occurred.

CONCLUSIONS

The results of an investigation of the effects of twist and camber with and without incidence, twist, and body indentation on a 45° swept-back wing-body configuration at Mach numbers from 0.80 to 1.03 and 1.15 indicate the following conclusions:

1. Negative incidence improved the values of maximum lift-drag ratios for the twisted and cambered wing-body configuration throughout the test Mach number range.
2. The effects of twist on the maximum lift-drag ratios were small when compared with those of twist and camber for Mach numbers through 1.03.

3. Twisting and cambering the wing increased the lift coefficient at which the unstable break in the pitching-moment curves occurred by approximately twice the amount of that for twist alone.

4. Body indentation increased the values of maximum lift-drag ratios for the twisted and cambered wing-body configuration at Mach numbers between 0.90 and 1.15 and increased the values of the maximum lift-drag ratios for the twisted wing-body configuration through Mach number 1.03.

5. The effects of twist and camber and body indentation at lift coefficients for maximum lift-drag ratios are additive at Mach numbers above 0.96.

Langley Aeronautical Laboratory,
National Advisory Committee for Aeronautics,
Langley Field, Va., January 27, 1954.

REFERENCES

1. Harrison, Daniel E.: A Transonic Wind-Tunnel Investigation of the Characteristics of a Twisted and Cambered 45° Sweptback Wing-Fuselage Configuration. NACA RM L52K18, 1952.
2. Jones, Robert T.: Estimated Lift-Drag Ratios at Supersonic Speeds. NACA TN 1350, 1947.
3. Morgan, Francis G., Jr., and Carmel, Melvin M.: Transonic Wind-Tunnel Investigation of the Effects of Taper Ratio, Body Indentation, Fixed Transition, and Afterbody Shape on the Aerodynamic Characteristics of a 45° Sweptback Wing-Body Combination. NACA RM L54A15, 1954.
4. Williams, Claude V., and Kuhn, Richard E.: A Study of the Aerodynamic Loads on Sweptback Wings at Transonic Speeds. NACA RM L53E08b, 1953.
5. Harrison, Daniel E.: The Influence of a Change in Body Shape on the Effects of Twist and Camber As Determined by a Transonic Wind-Tunnel Investigation of a 45° Sweptback Wing-Fuselage Configuration. NACA RM L53B03, 1953.
6. Robinson, Harold L.: A Transonic Wind-Tunnel Investigation of the Effects of Body Indentation, As Specified by the Transonic Drag-Rise Rule, on the Aerodynamic Characteristics and Flow Phenomena of a 45° Sweptback-Wing-Body Combination. NACA RM L52L12, 1953.
7. Whitcomb, Richard T.: A Study of Zero-Lift Drag-Rise Characteristics of Wing-Body Combinations Near the Speed of Sound. NACA RM L52H08, 1952.
8. Williams, Claude V.: A Transonic Wind-Tunnel Investigation of the Effects of Body Indentation, As Specified by the Transonic Drag-Rise Rule, on the Aerodynamic Characteristics and Flow Phenomena of an Unswept-Wing-Body Combination. NACA RM L52L23, 1953.

TABLE I.- COORDINATES OF BASIC AND INDENTED BODIES

Basic body		Indented body	
Station, in.	Radius, in.	Station, in.	Radius, in.
0	0	0	0
.225	.104	.225	.104
.3375	.134	.3375	.134
.5625	.193	.5625	.193
1.125	.325	1.125	.325
2.250	.542	2.250	.542
3.375	.726	3.375	.726
4.500	.887	4.500	.887
6.750	1.167	6.750	1.167
9.000	1.390	9.000	1.390
11.250	1.559	11.250	1.559
13.500	1.683	13.500	1.683
15.750	1.770	15.750	1.770
18.000	1.828	18.000	1.828
20.250	1.864	20.250	1.864
22.500	1.875	22.500	1.875
23.000	1.875	23.125	1.874
23.692	1.875	23.625	1.864
24.192	1.875	24.125	1.825
24.692	1.875	24.625	1.812
25.192	1.875	25.125	1.771
25.692	1.875	25.625	1.742
26.192	1.875	26.125	1.701
26.692	1.872	26.625	1.650
27.192	1.871	27.125	1.626
27.692	1.868	27.625	1.595
28.192	1.866	28.125	1.568
28.692	1.862	28.625	1.551
29.192	1.856	29.125	1.541
29.692	1.849	29.625	1.537
30.192	1.839	30.125	1.537
30.692	1.825	30.625	1.537
31.192	1.808	31.125	1.536
31.692	1.789	31.625	1.530
32.192	1.768	32.125	1.517
32.692	1.745	32.675	1.499
33.192	1.720	33.125	1.482
33.692	1.694	33.625	1.472
34.192	1.667	34.125	1.468
34.692	1.638	34.625	1.468
35.192	1.608	35.125	1.468
35.692	1.570	35.625	1.468
36.192	1.531	36.125	1.468
36.692	1.486	36.625	1.468
36.900	1.467	36.900	1.467
37.500	1.408	37.500	1.408
38.000	1.355	38.000	1.355
38.500	1.298	38.500	1.298
39.000	1.235	39.000	1.235
39.500	1.167	39.500	1.167
40.000	1.100	40.000	1.100
40.500	1.030	40.500	1.030
41.250	.937	41.250	.937

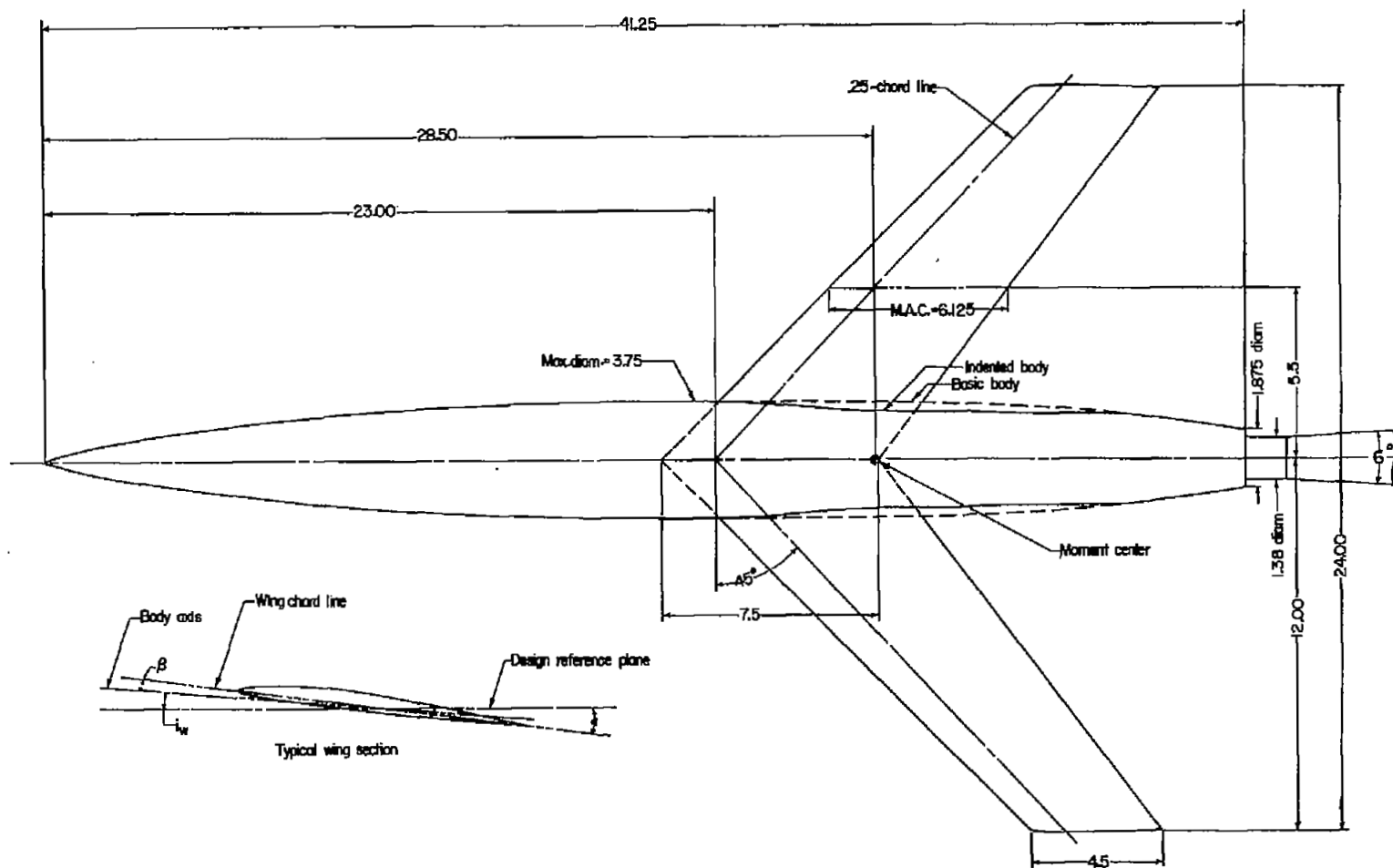


Figure 1.- Plan view of wing-body configurations with typical wing section showing angle of incidence α_w and angle of twist ϵ . All dimensions are in inches.

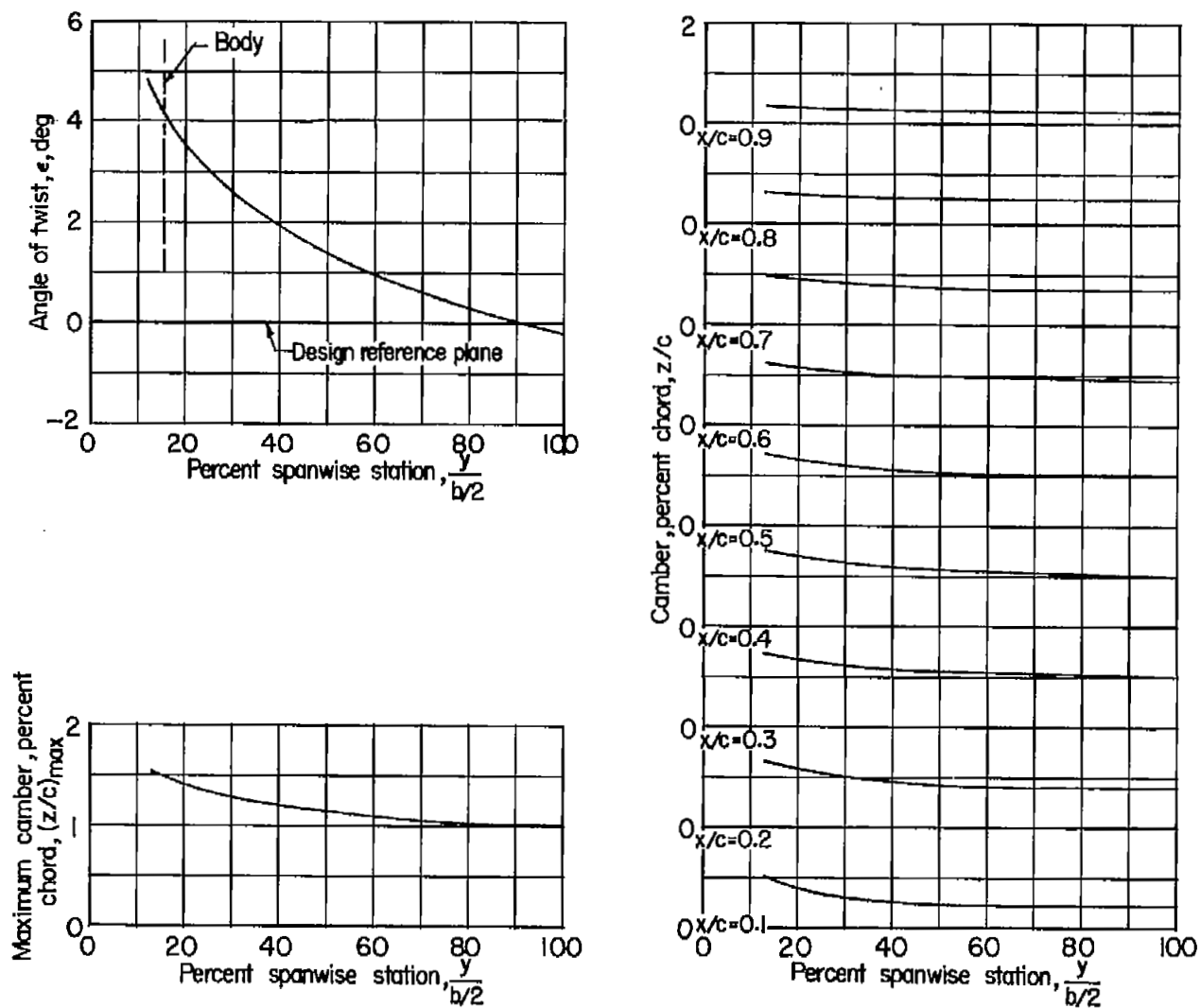


Figure 2.- Spanwise variation of the twist and camber of the twisted and cambered wing.

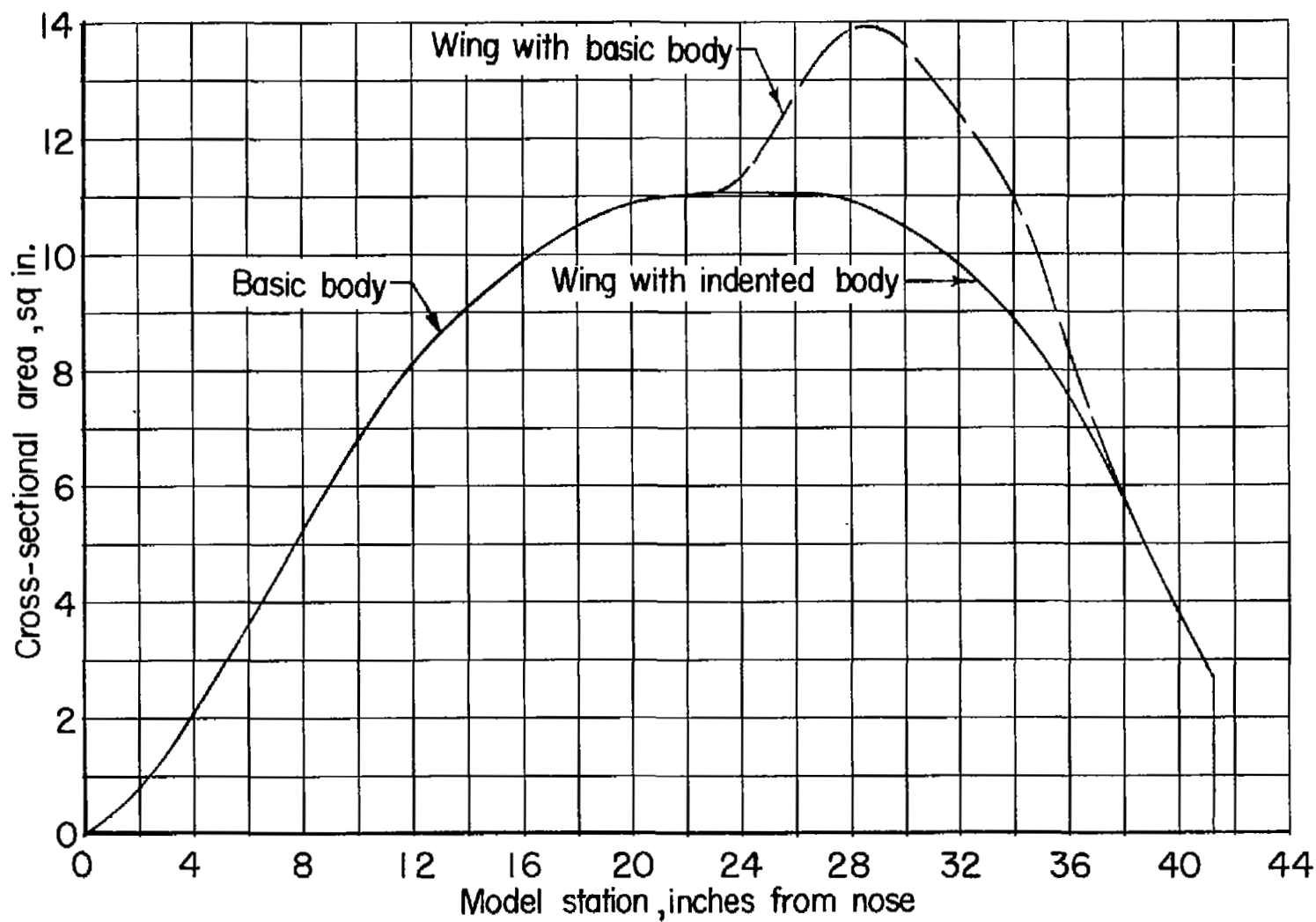


Figure 3.- Axial distributions of cross-sectional area for wing in combination with the indented body and the basic body.

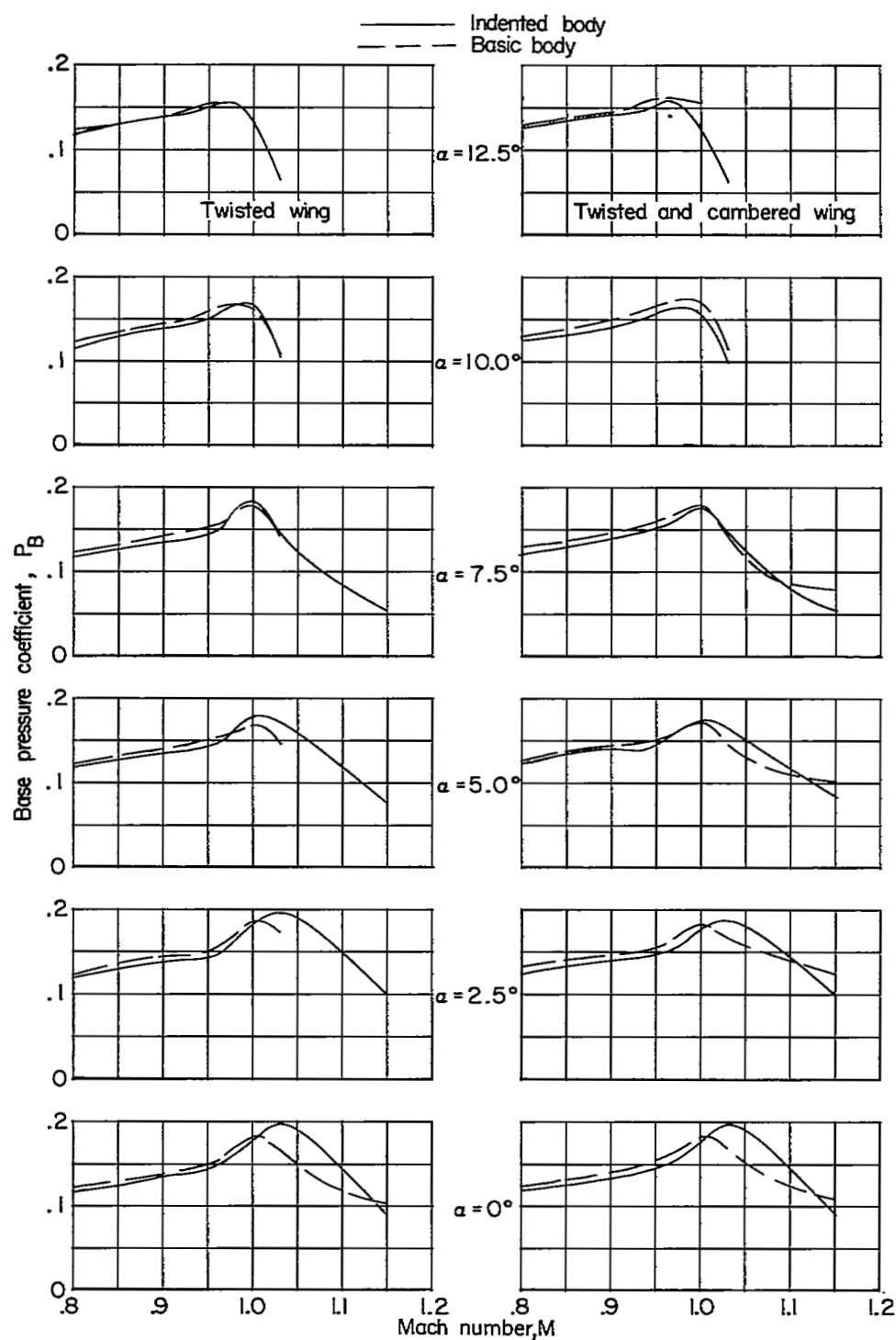
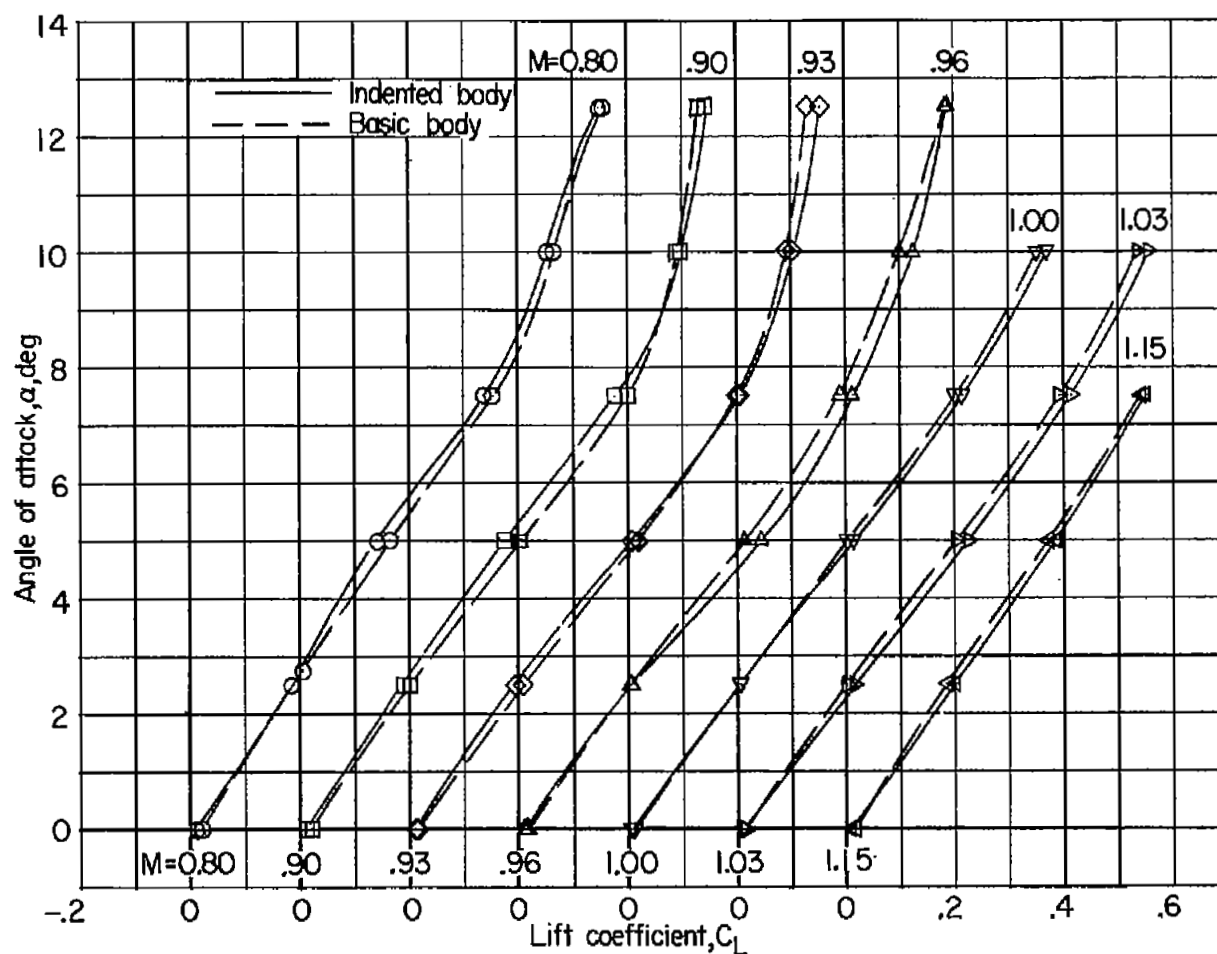
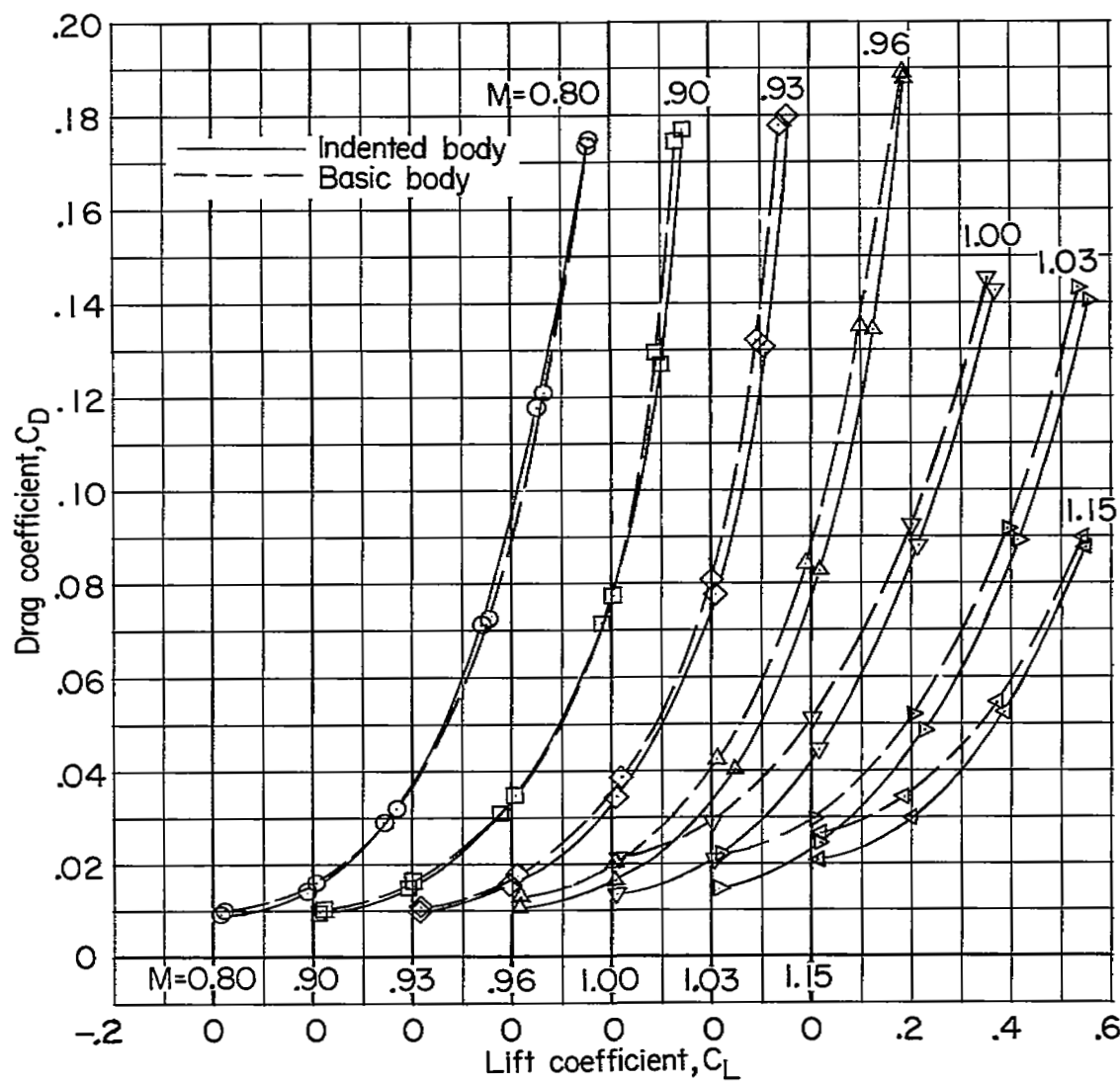


Figure 4.- Base pressure coefficients for the twisted, and twisted and cambered wing-body configurations. $i_w = -4^\circ$.



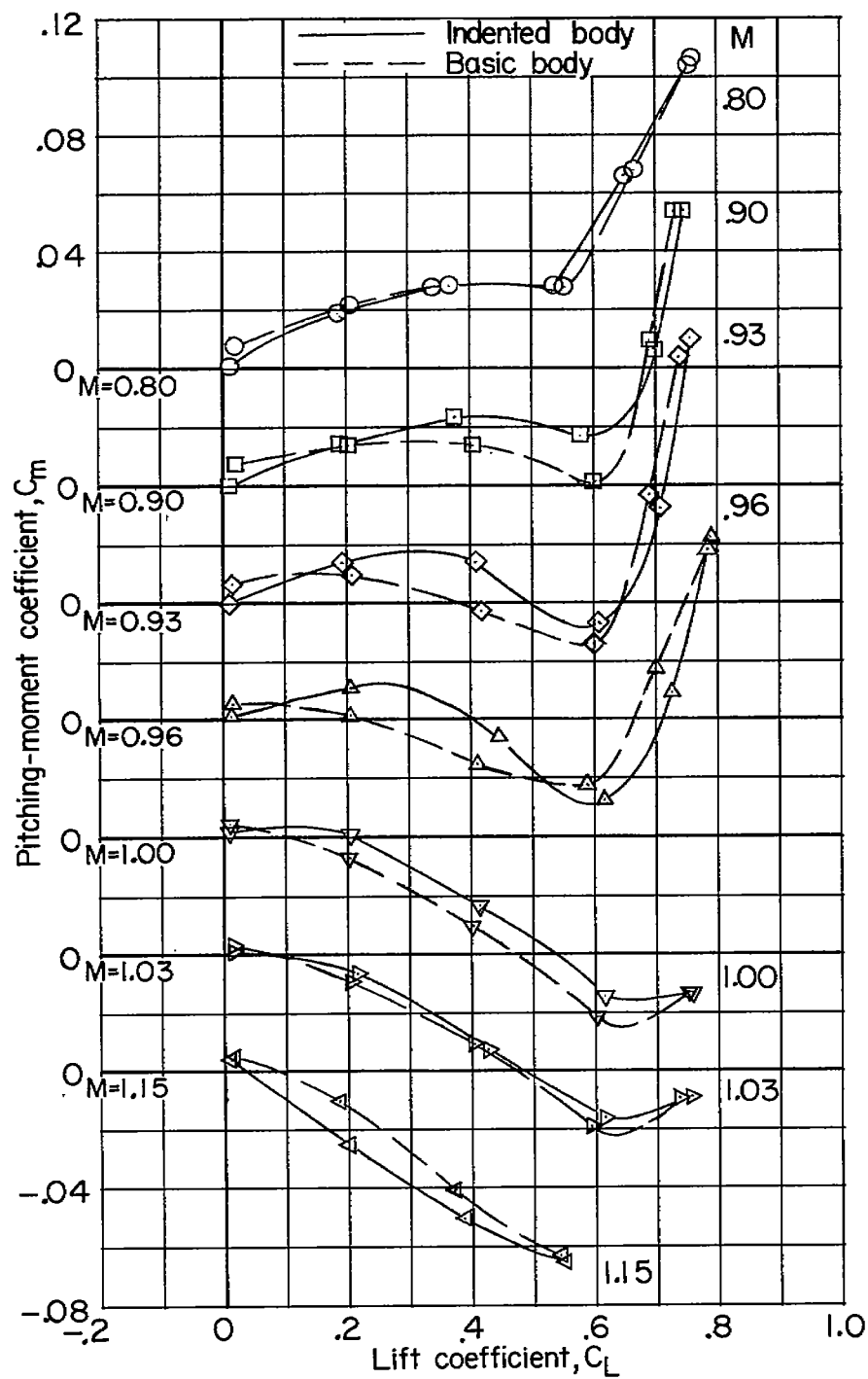
(a) Angle of attack.

Figure 5.- Variation with lift coefficient of the aerodynamic characteristics for the plane wing-body configurations. $i_w = 0^\circ$ (ref. 3).



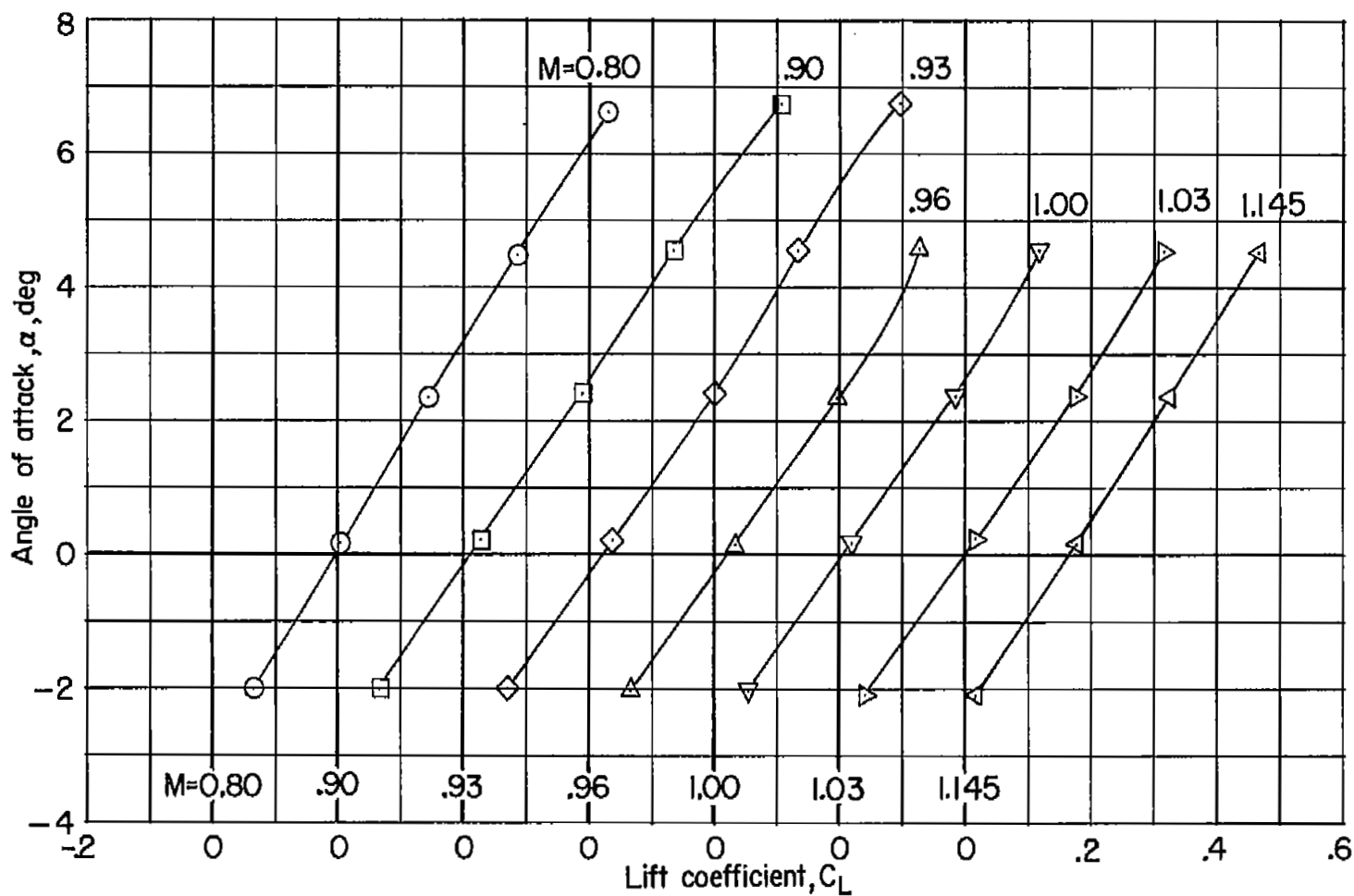
(b) Drag coefficient.

Figure 5.- Continued.



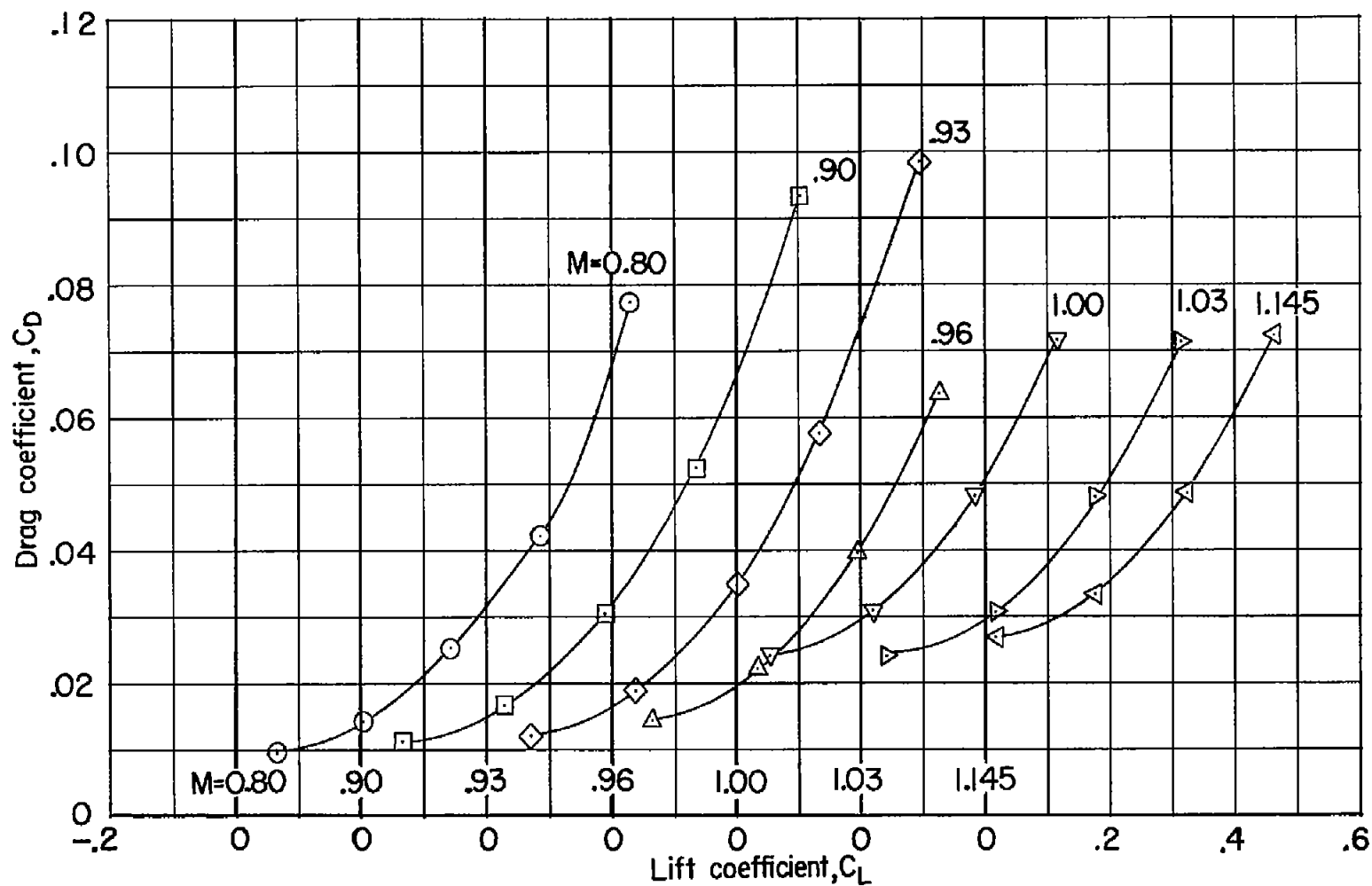
(c) Pitching-moment coefficient.

Figure 5.- Concluded.



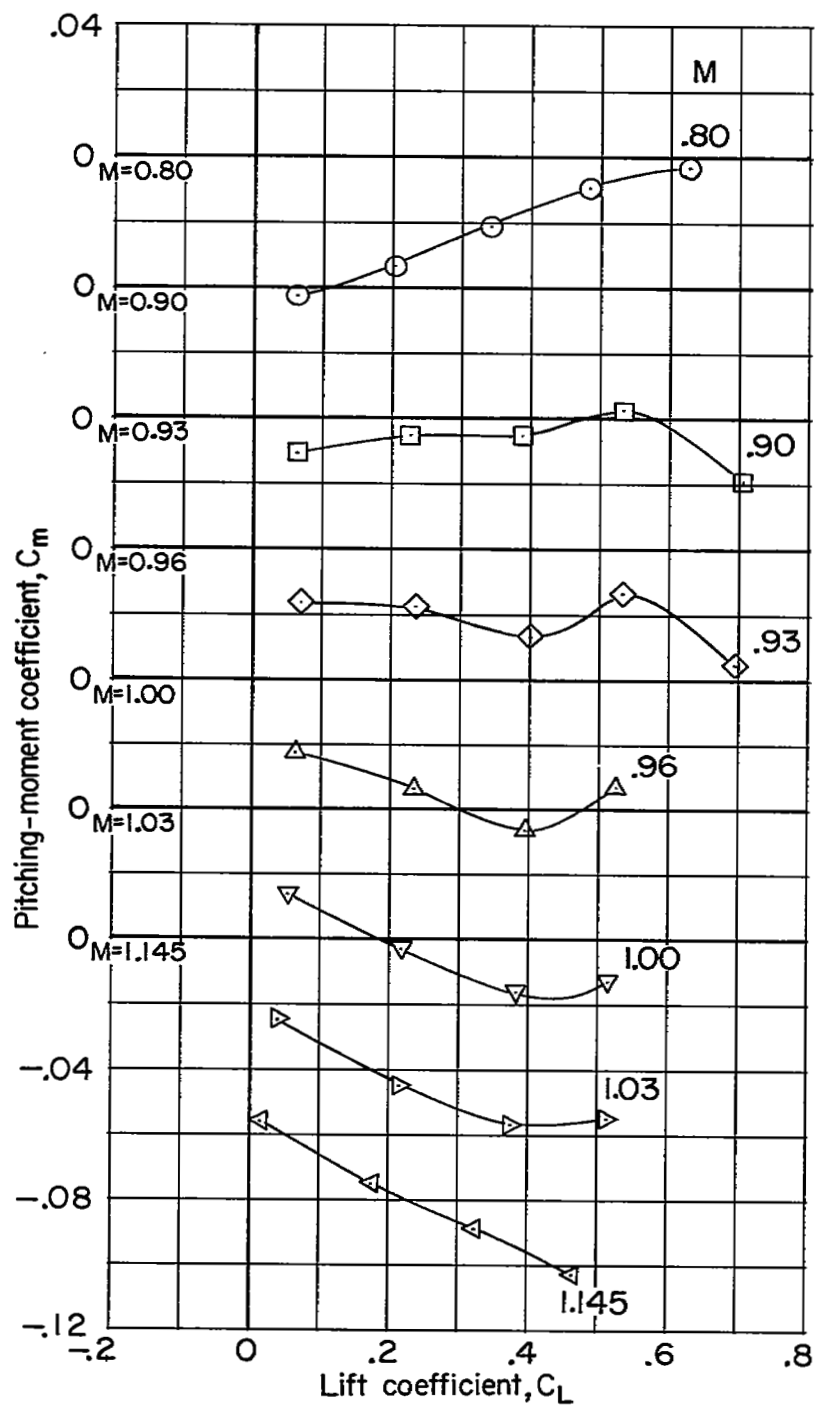
(a) Angle of attack.

Figure 6.- Variation with lift coefficient of the aerodynamic characteristics for the twisted and cambered wing--basic-body configuration. $i_w = 0^\circ$.



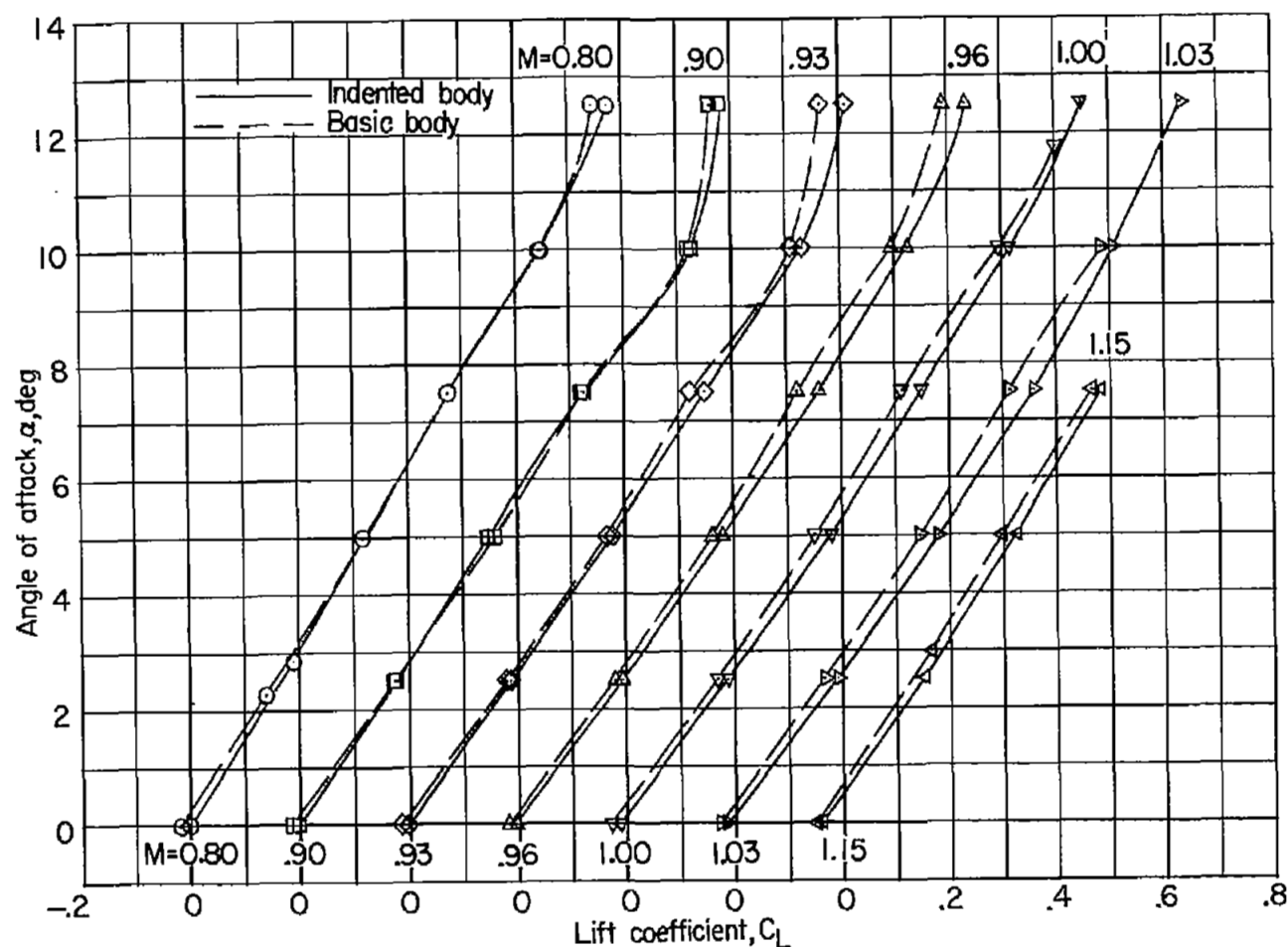
(b) Drag coefficient.

Figure 6.- Continued.



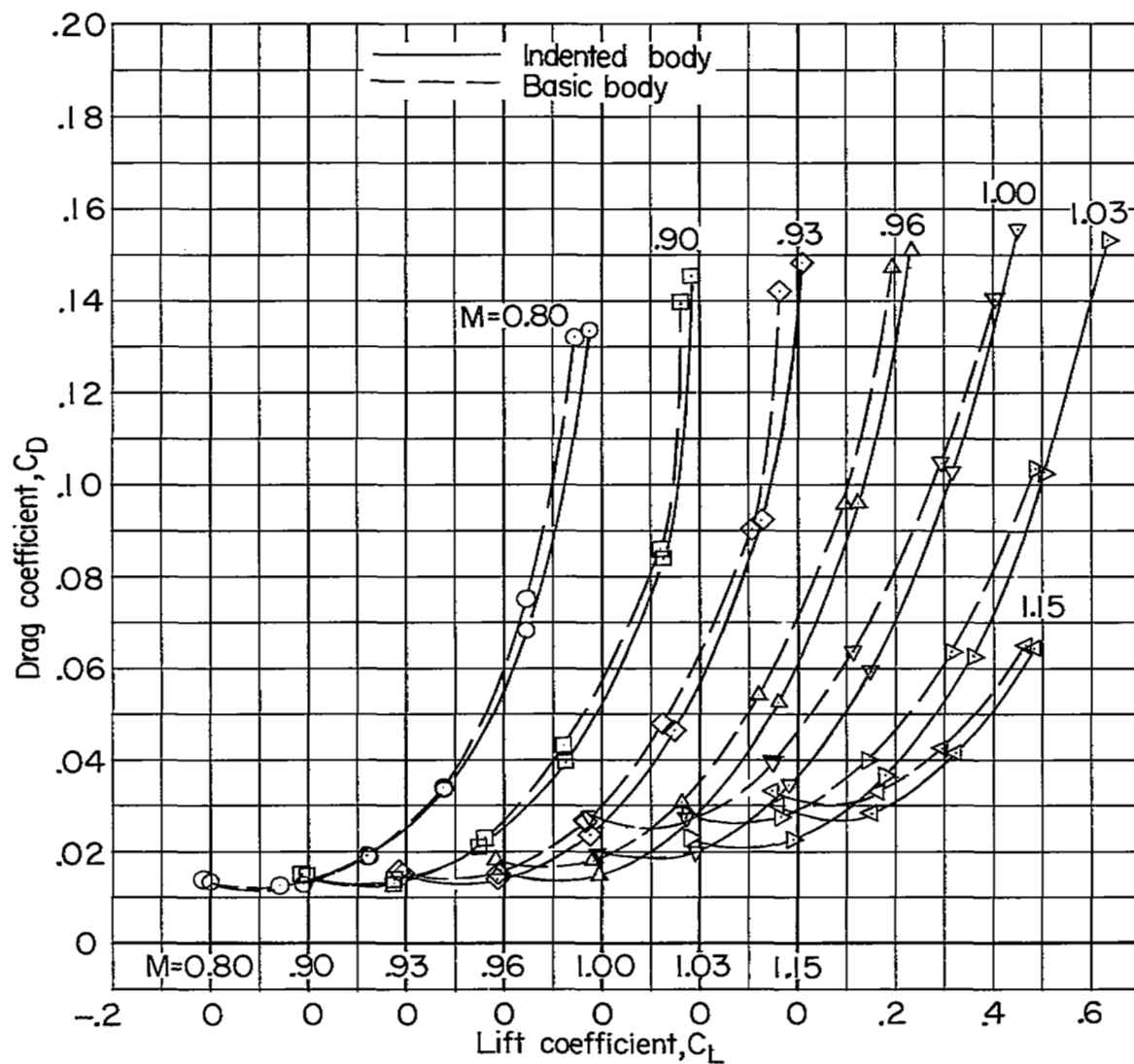
(c) Pitching-moment coefficient.

Figure 6.- Concluded.



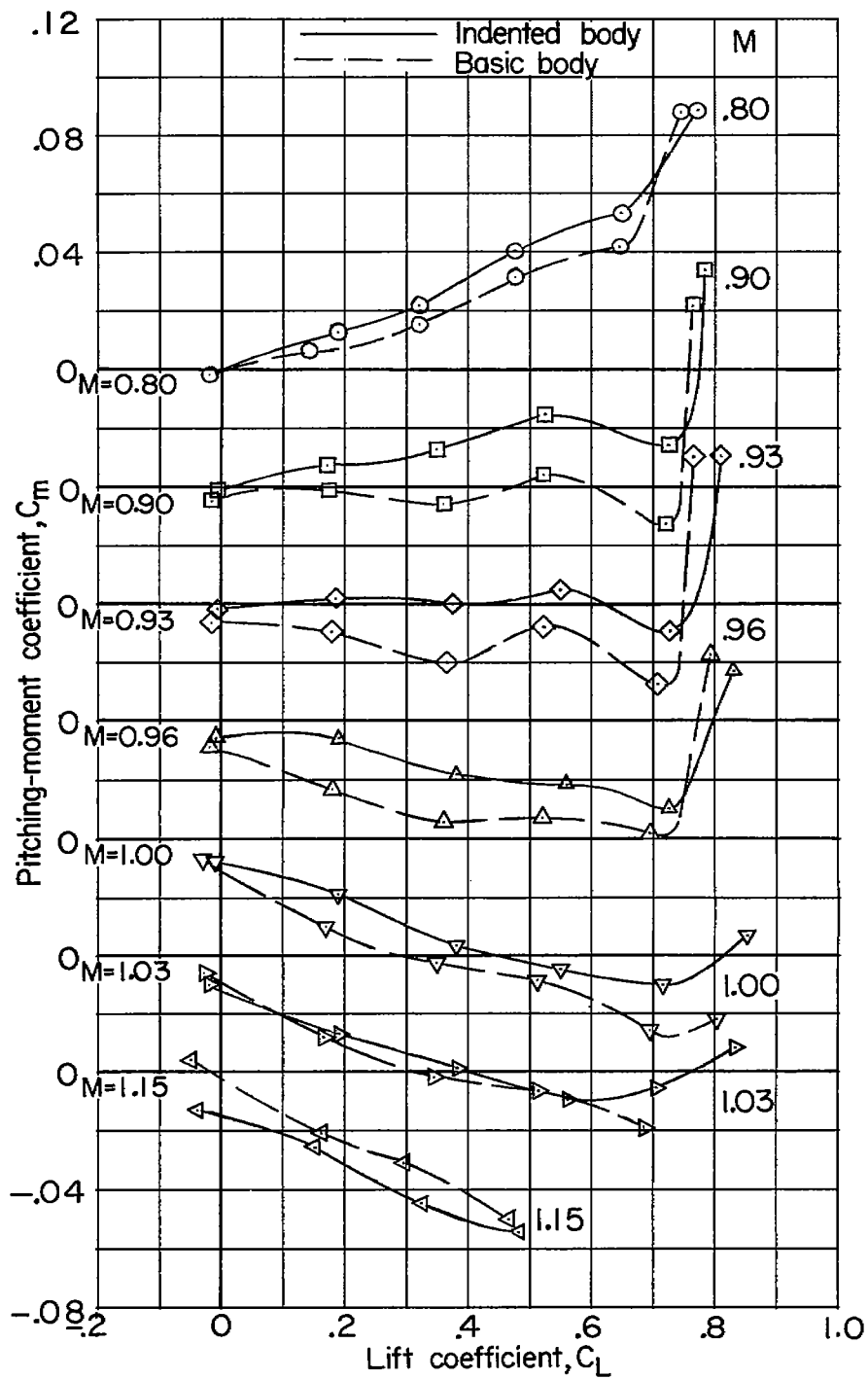
(a) Angle of attack.

Figure 7.- Variation with lift coefficient of the aerodynamic characteristics for the twisted and cambered wing-body configurations. $i_w = -4^\circ$.



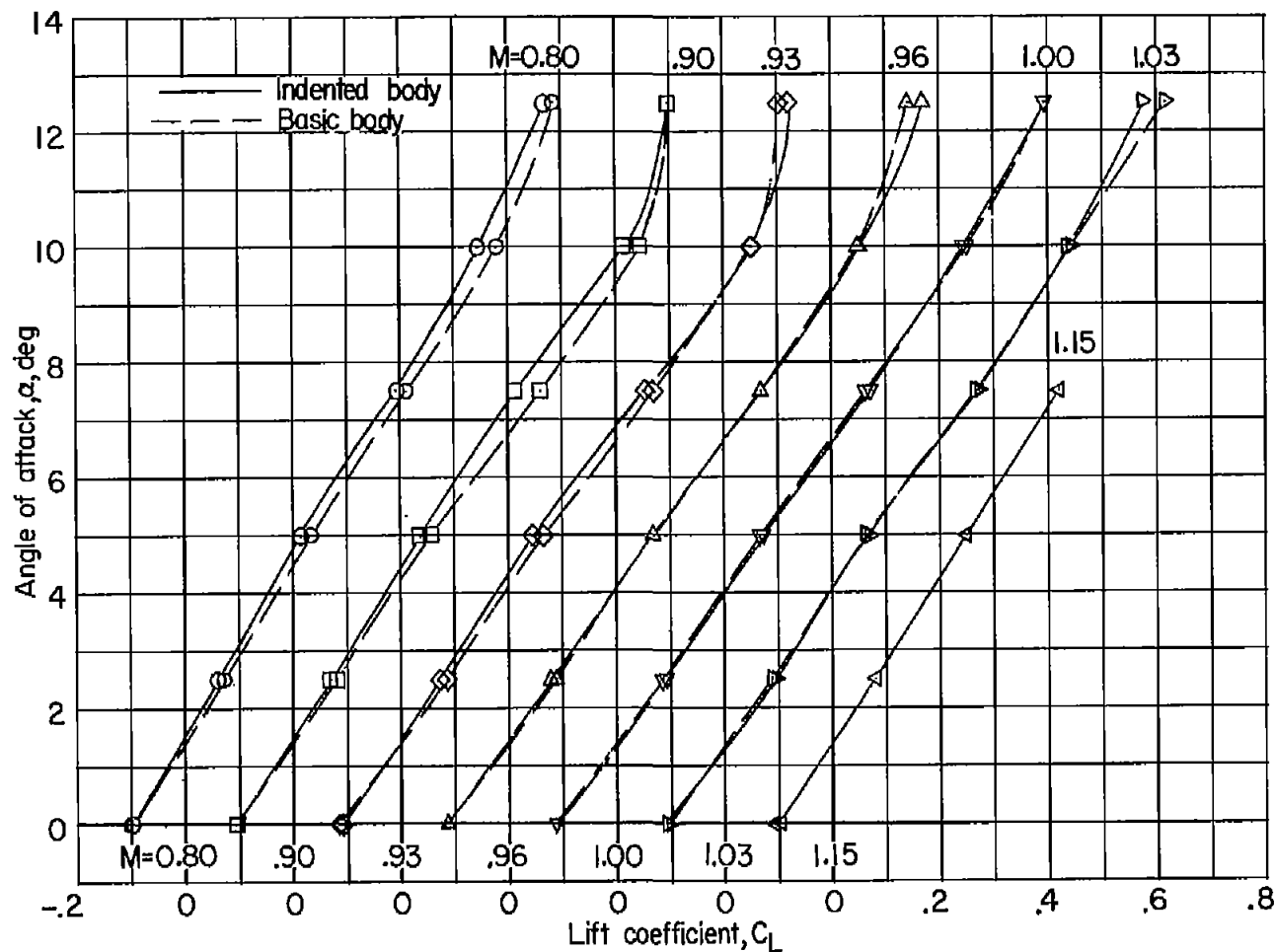
(b) Drag coefficient.

Figure 7.- Continued.



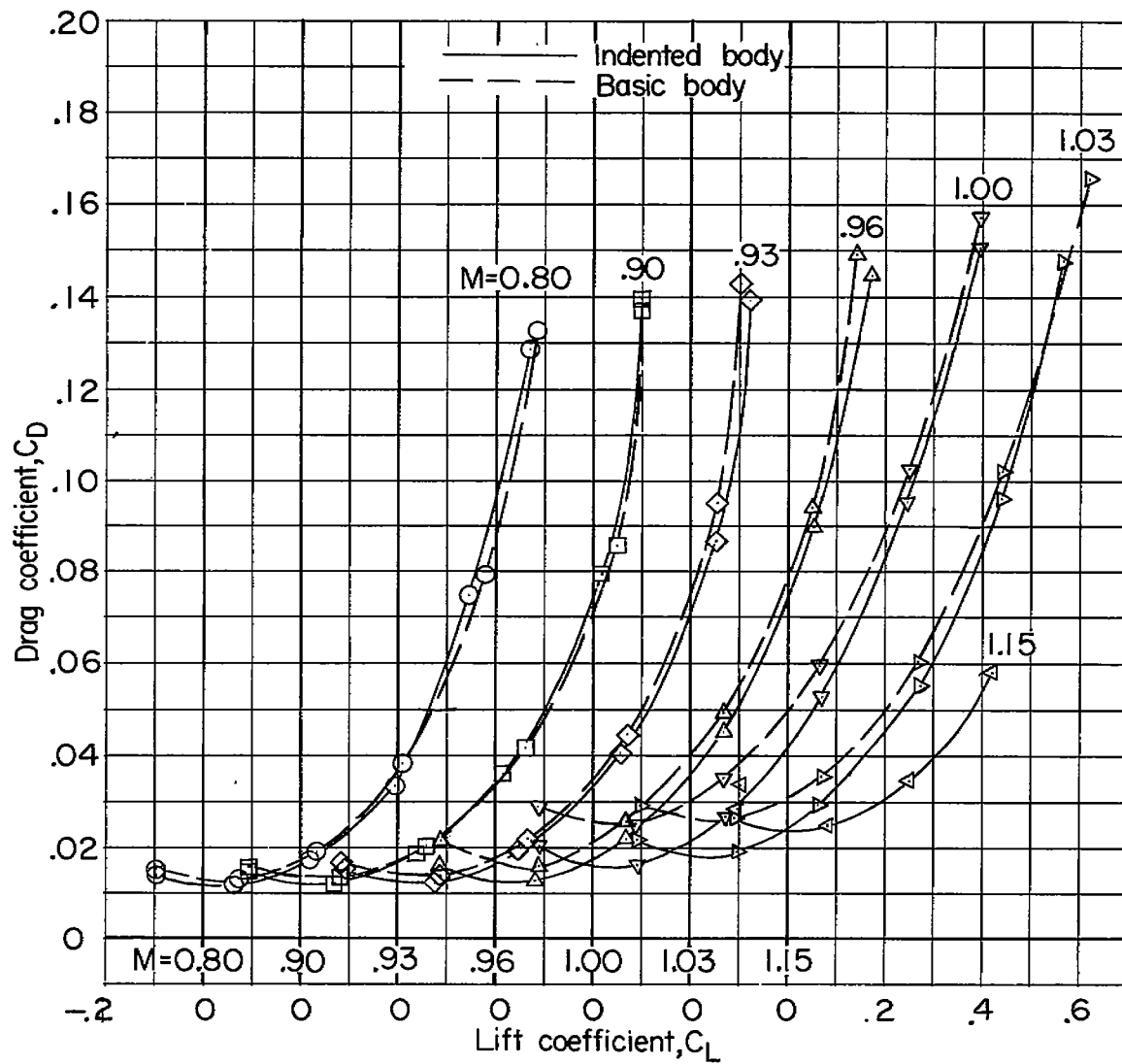
(c) Pitching-moment coefficient.

Figure 7.- Concluded.



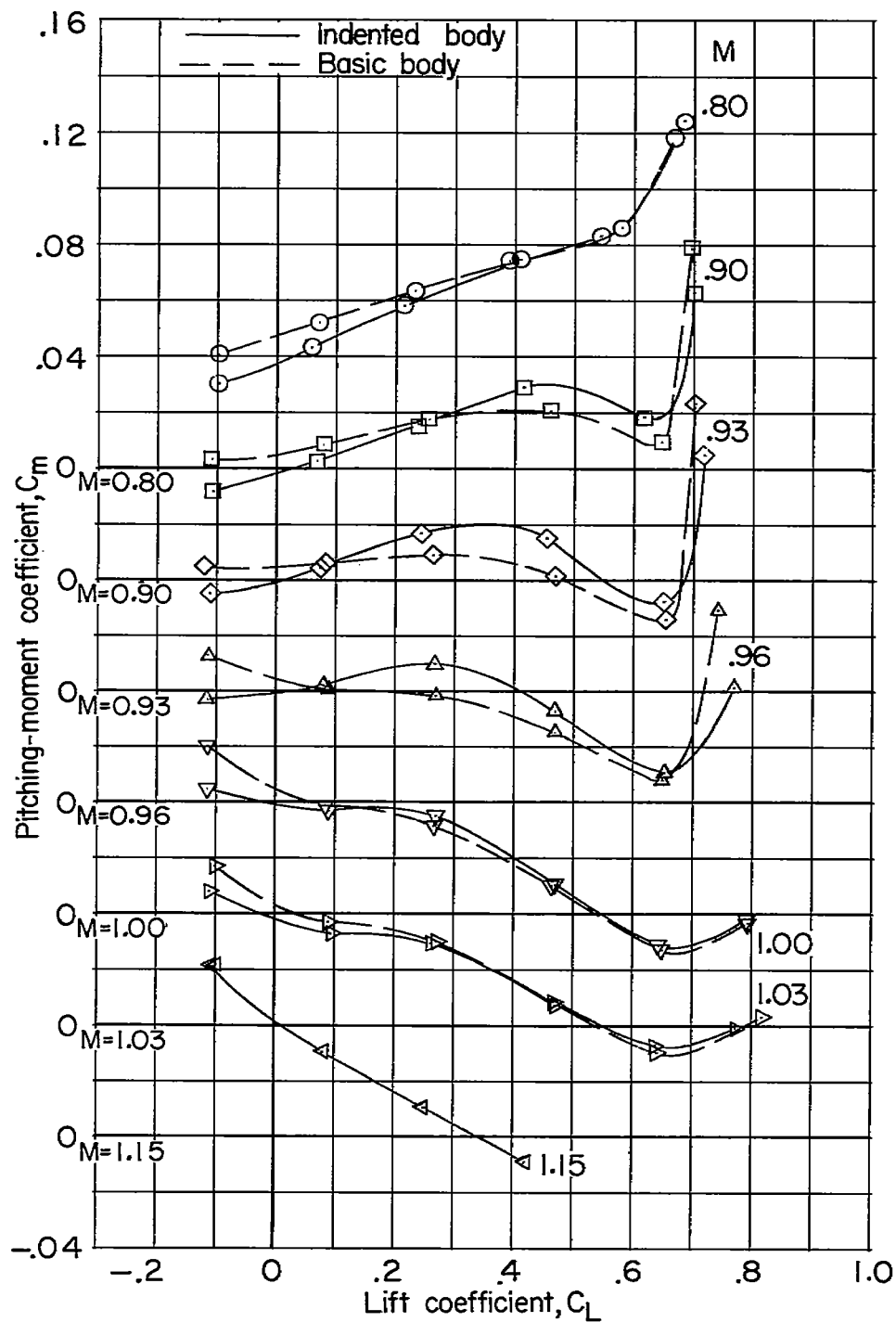
(a) Angle of attack.

Figure 8.- Variation with lift coefficient of the aerodynamic characteristics for the twisted wing body configurations. $i_w = -4^\circ$.



(b) Drag coefficient.

Figure 8.- Continued.



(c) Pitching-moment coefficient.

Figure 8.- Concluded.

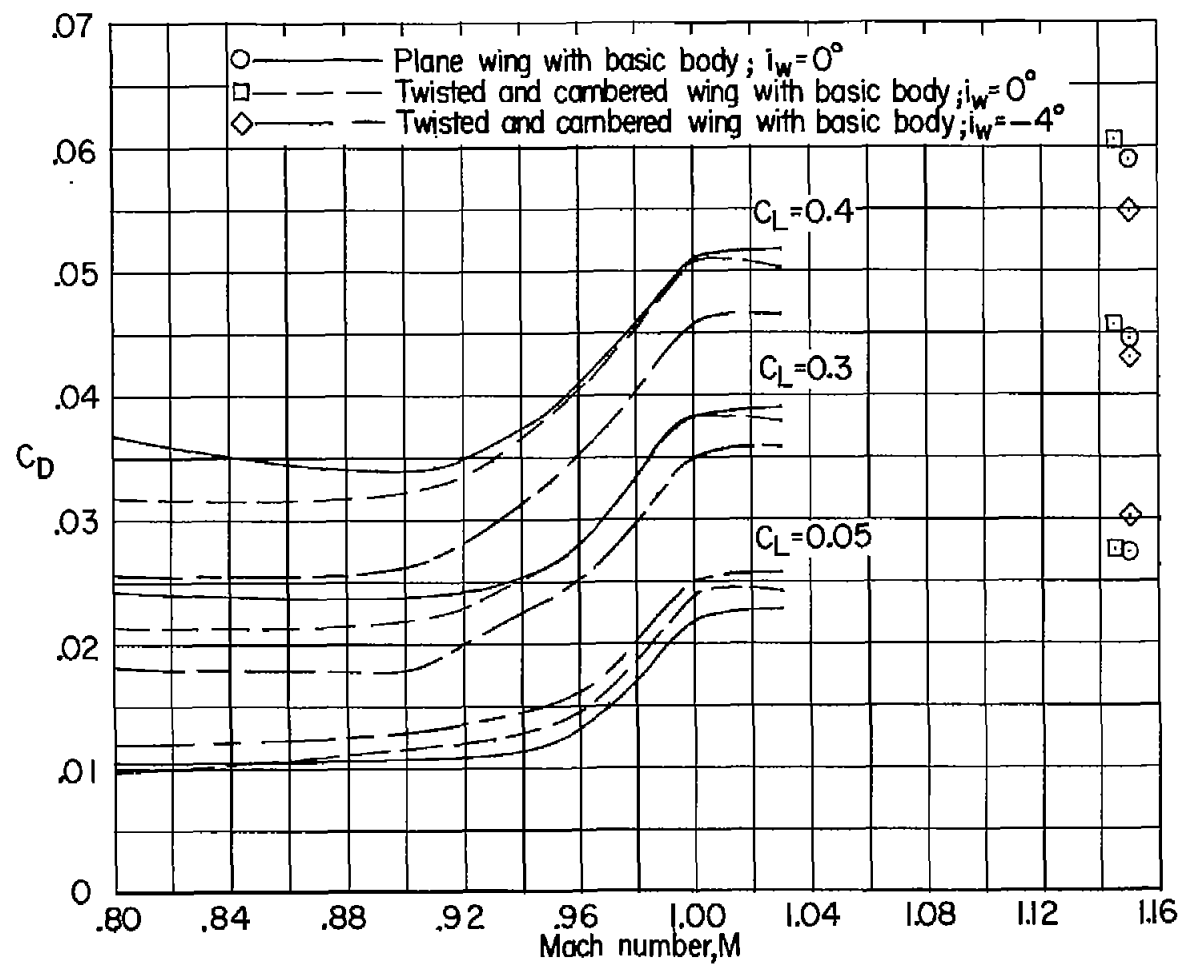


Figure 9.- Variation of drag coefficient with Mach number at constant lift coefficient for the plane wing—basic-body configuration without incidence, and the twisted and cambered wing—basic-body configuration with and without incidence.

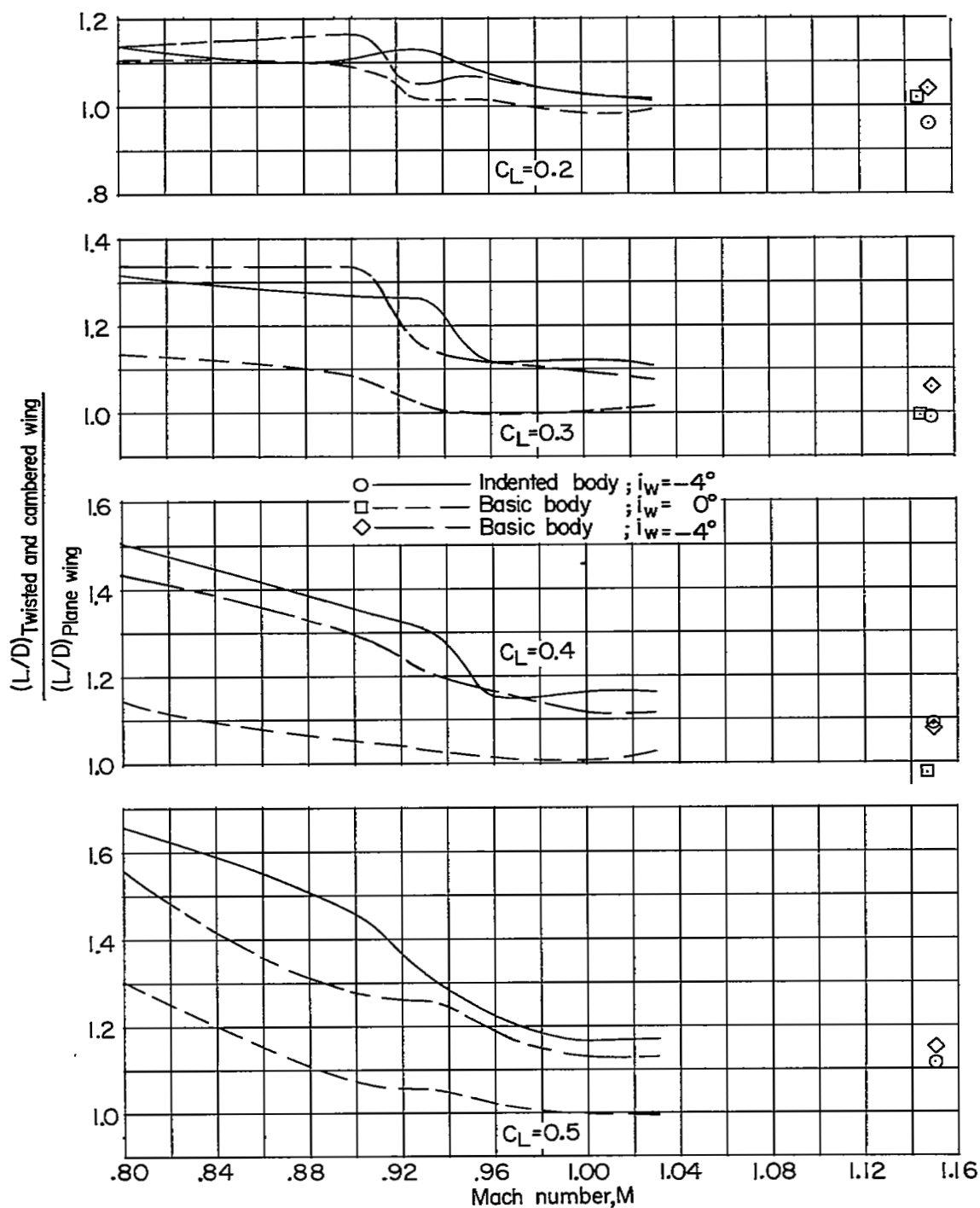


Figure 10.- Effect of twist and camber on the values of L/D at constant lift coefficient for the wing-indentured-body configuration with incidence and the wing-basic-body configuration with and without incidence.

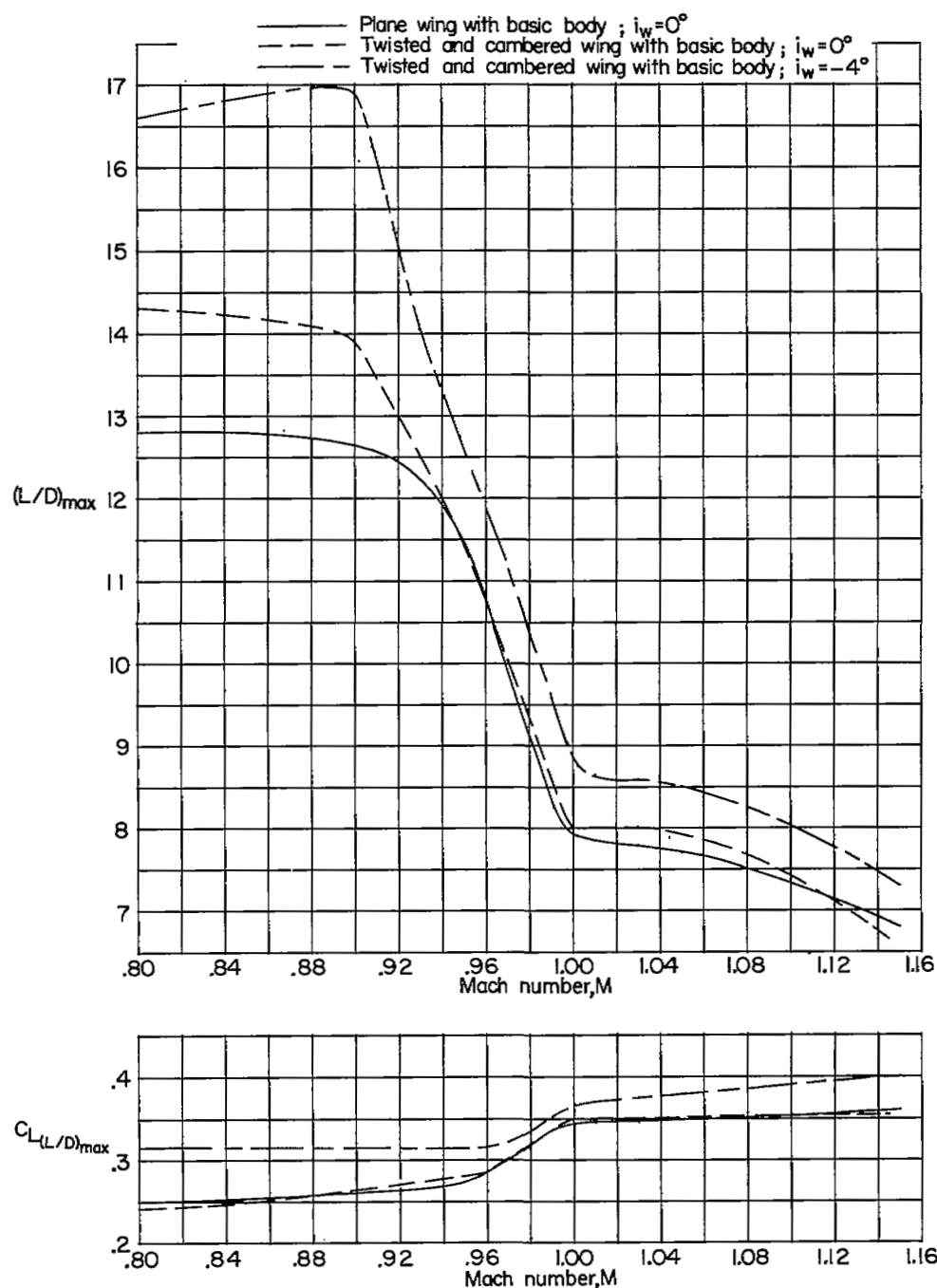


Figure 11.- Variation of the maximum lift-drag ratios with Mach number for the plane wing—basic-body configuration without incidence and the twisted and cambered wing—basic-body configuration with and without incidence.

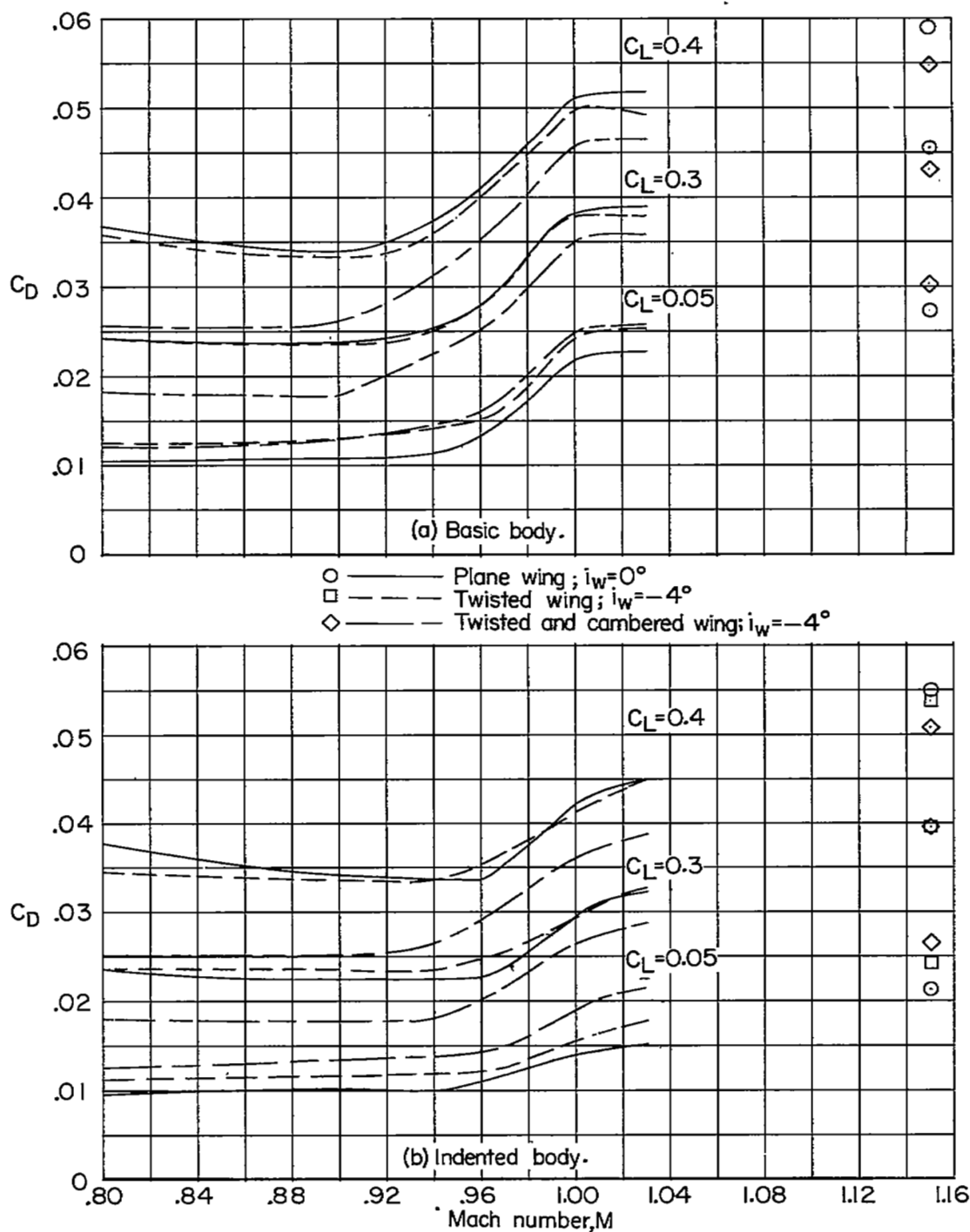


Figure 12.- Variation of drag coefficient with Mach number at constant lift coefficient for the plane, twisted, and twisted and cambered wing-body configurations with basic and indented bodies.

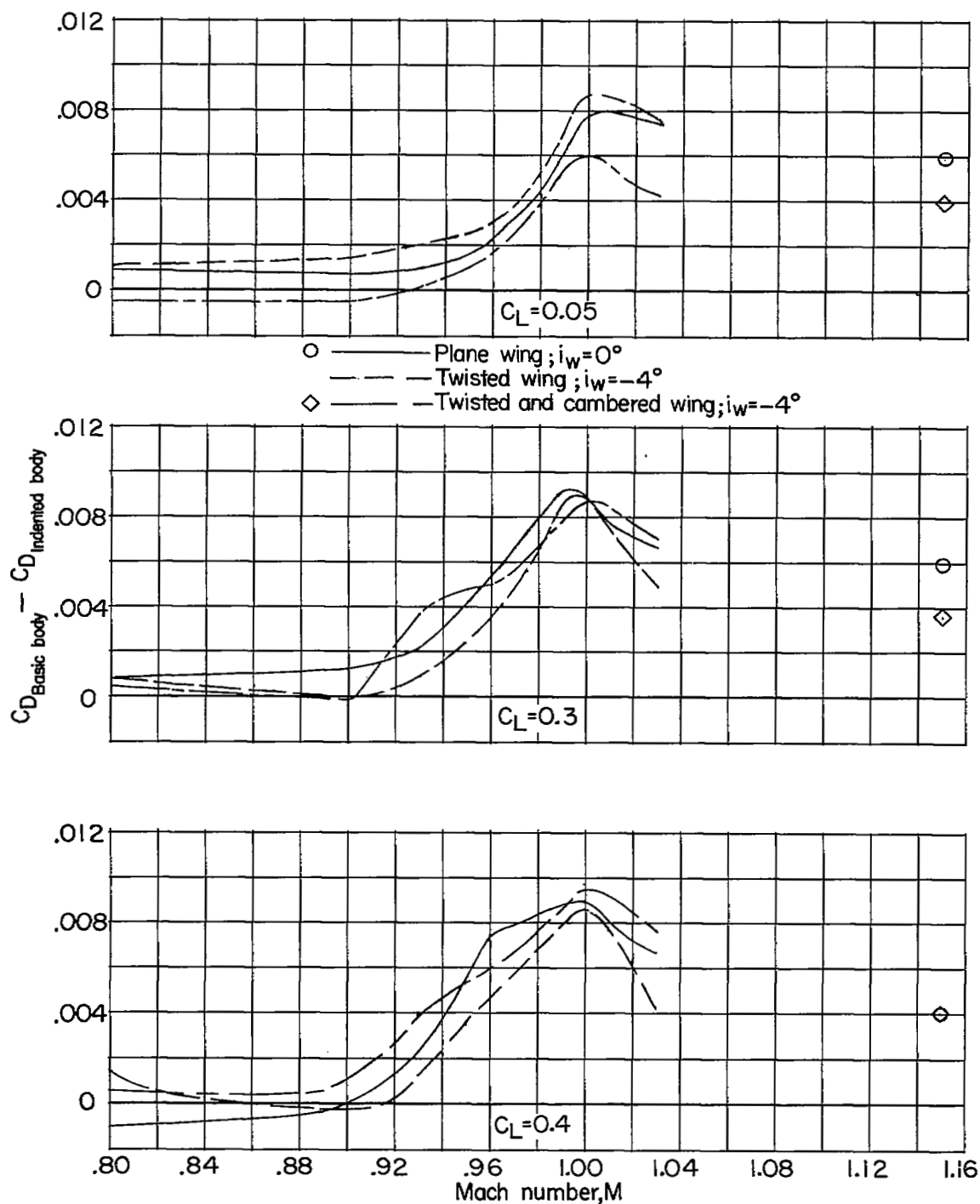


Figure 13.- Variation of the effect of body indentation with Mach number at constant lift coefficient for the plane, twisted, and twisted and cambered wing-body configurations.

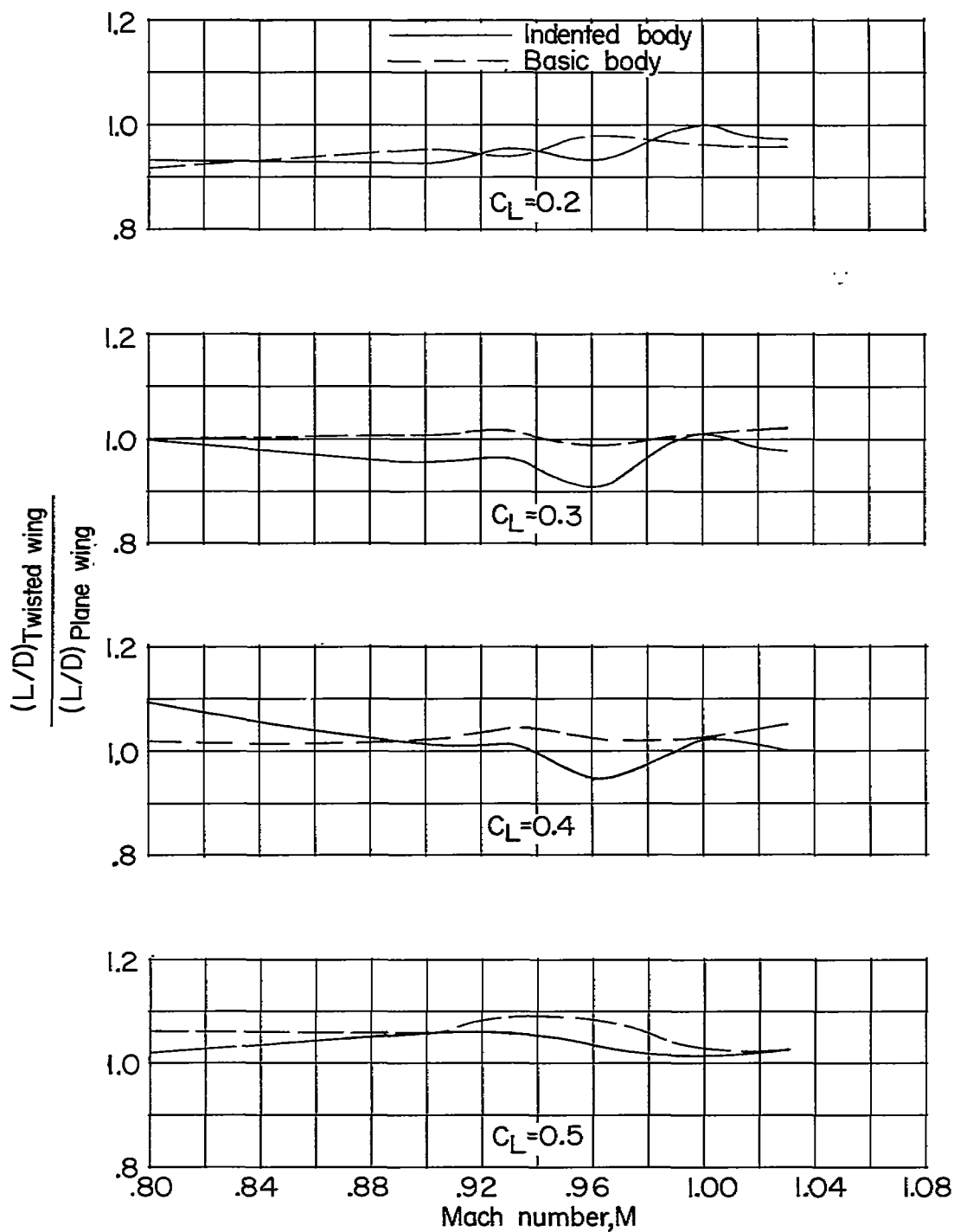


Figure 14.- Effect of twist on the values of L/D at constant lift coefficient for the wing-indent-ed-body and the wing-basic-body configurations. $i_w = -4^\circ$.

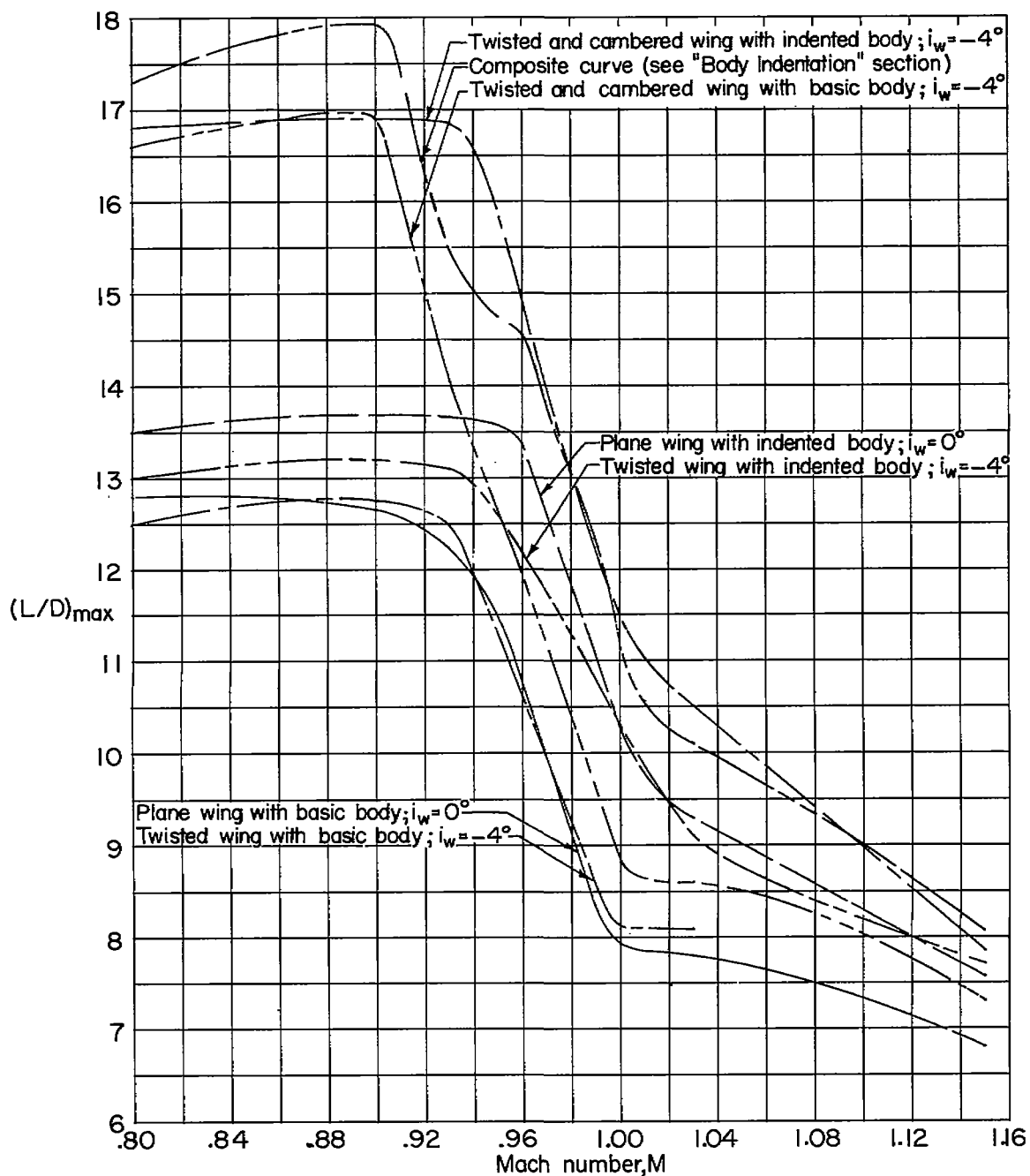


Figure 15.- Variation of the maximum lift-drag ratios with Mach number for the plane, twisted, and twisted and cambered wing-body configurations with indented and basic bodies.

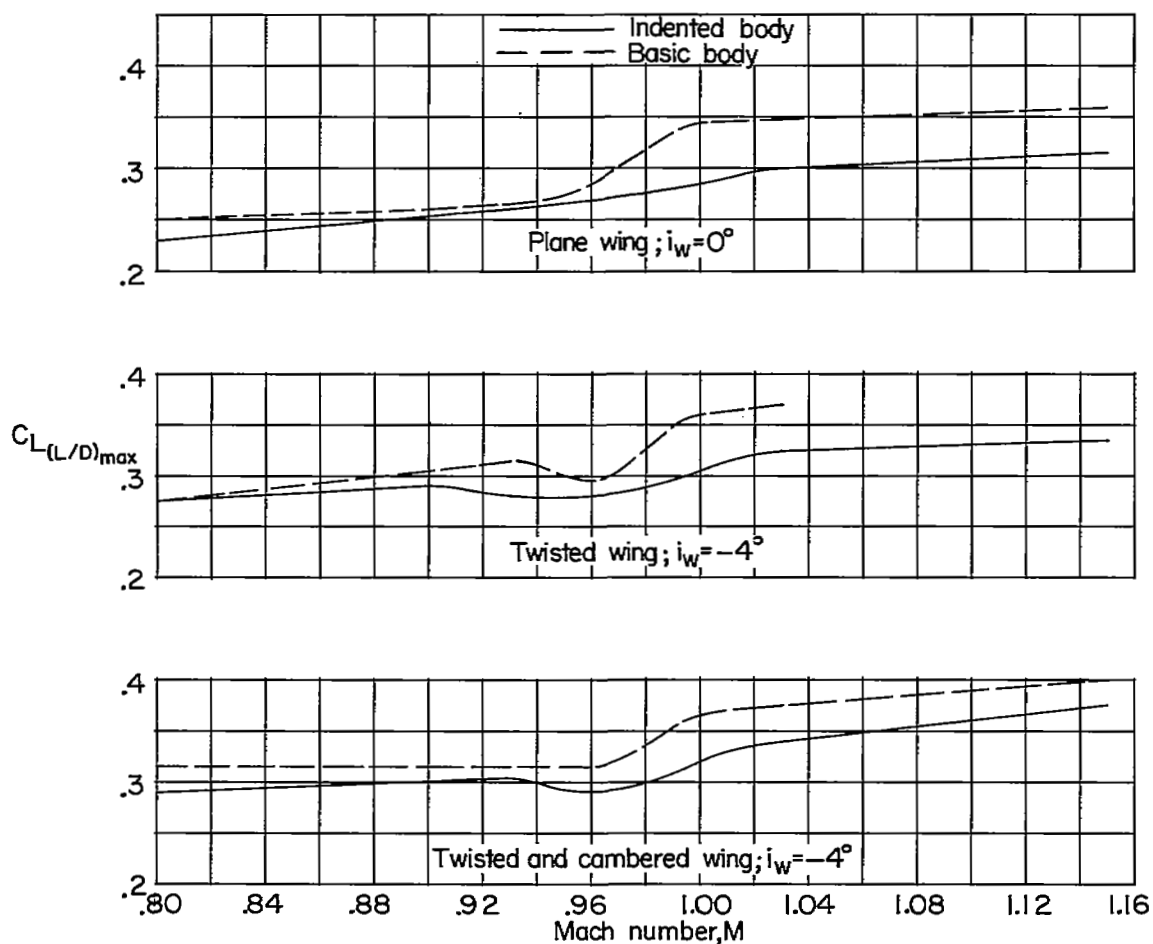


Figure 16.- Lift coefficients at which the maximum lift-drag ratios were obtained for the plane, twisted, and twisted and cambered wing-body configurations with indented and basic bodies.

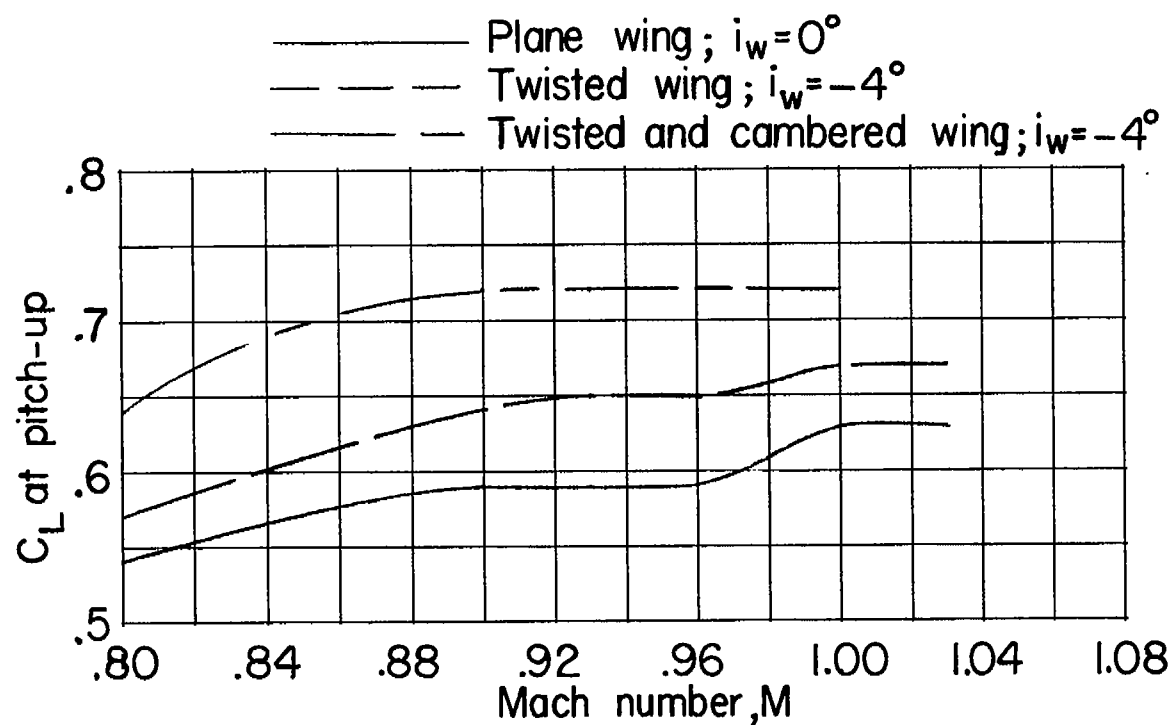


Figure 17.- Lift coefficients at which the unstable break in the pitching-moment curves occurred for the plane, twisted, and twisted and cambered wing-body configurations with indented and basic bodies.

[REDACTED]

NASA Technical Library



3 1176 01437 1331

[REDACTED]

[REDACTED]